NUMERICAL SIMULATION OF THE PLASTICS INJECTION MOULDING PROCESS USING A THIN GAP NUMERICAL MODEL

CLINTON VAN LINGEN KIETZMANN, B. Ing. (Mechanical Engineering)

Thesis accepted in the Faculty of Engineering of the Potchefstroom University for Christian Higher Education in partial fulfilment of the requirements for the degree Magister Ingenieurswese in Mechanical Engineering.

Supervisor: Prof. G.P. Greyvenstein

POTCHEFSTROOM

June 1995

1 INTRODUCTION

1.1 Introduction

1.1.1 Background

Injection moulding is a process with which thermoplastic materials are converted into useful end products. It is the most practical and rapid method of producing articles of intricate shape. The material, usually in the form of small pellets, is heated up in the chamber of the machine and not in the mould itself. As the material liquifies, a plunger compresses it and forces it to emerge through a nozzle into a cold mould, where the pressure causes it to take the shape of the cavity. The material cools rapidly in the mould, usually aided by an external cooling medium, and when rigid, is automatically ejected as the mould opens. Typical products of this process are combs, brush handles, pens and many other articles in everyday use.

Never before have the skills of the part designer and the mould designer been so stretched. The use of plastics as a manufacturing material in original design or metal replacement offers designers tremendous scope for additional function and cost saving. But although the best designers' knowledge may have been applied to a particular problem the resultant moulding can still fall short of expectations in, for example, distortion, poor surface finish, or less visible defects such as built in stresses, and even moulds that refuse to fill properly.

The traditional approach to these problems is for the moulder to allow a trial period after the mould has been completed for rectification of any problems. This process is not only costly and time consuming, but also frustrating for the customer waiting to see his new parts.

Over the past several years Computational Fluid Dynamics (CFD) along with inexpensive computing has come to the fore. The CFD program simulates the filling and holding processes of injection

moulding on a computer enabling the designer to see whether the mould will fill and pack properly. Clearly any tool that can help designers predict and verify the mouldability of a part before cutting the metal can eliminate the expense of reworking tools and slipping schedules.

1.1.2 Injection moulding process

The injection moulding process can be divided into three major stages filling, packing and cooling. During the filling stage the pressure in the mould rises slowly, as the molten non-Newtonian, compressible polymer spreads to fill the empty cold cavity. The flow is unsteady and the polymer starts cooling as soon as it touches the cold walls of the mould. Polymer flow into the cavity does not cease when the melt reaches the outer boundaries, but more polymer is forced into the mould during the packing stage to compensate for shrinkage during the cooling stage which at first runs simultaneously with the packing stage.

1.1.3 Simulation of the injection moulding process

It can be said that the major advance in the design and manufacture of injection moulds has been due to advances in computer simulations of the injection moulding process. Such packages assist in

i) determining the appropriate number and location of gates (small openings in the cavity through which the injected material enters the cavity),

ii) sizing the length and cross sectional area of the runner system (channel like members, typically either trapezoidal or semi circular in shape, through which the injected material gets delivered to the gate from the upstream screw-injection machine),

iii) locating vents in the cavity preventing scorching which can occur if the displaced air gets trapped and heated up due to compression and

iv) determining appropriate processing conditions for the given material and mould.

In general the intent of such computer-assisted designs is to fill the cavity uniformly and so doing preventing premature filling of any portion of the cavity which can cause over-packing and result in non-uniform dimensional stability and mechanical properties of the final moulded part. In addition such designs are subject to certain constraints such as the maximum available clamp force of the machine. If the force generated by the pressure inside the mould exceeds the maximum force then flashing occurs. Flashing amounts to the partial opening of the cavity with attendant spilling out of the supposedly sealed mould. Computer simulations also assist predicting the positions of the weld lines in the final moulded product. Weld lines are formed when two melt fronts impinge upon each other which occur when the molten plastic has to flow around an insert in the mould or when the mould is filled from two different gates. Such weld lines are an unpleasant sight and harm the aesthetic value of the moulded part. These weld lines also indicate local diminished mechanical strength and are stress concentrations.

Filling is usually simulated as a transient, isothermal or non-isothermal flow of a laminar non-Newtonian incompressible fluid, with a moving free surface. Finite-difference or finite element methods are usually used and several flow analysis programs for molten polymers are now commercially available (eg Moldflow, C-Flow, Cadmold, Timon, Simuflow, Procop, Polyflow) Most of them exist as part of an integrated CAD/CAM/CAE package and are primarily intended to facilitate and automate mould design. Due to the programs being integrated with other packages they are usually dependant on the type of machine that does the injection moulding. Most of the commercial packages operate on expensive work stations and are thus beyond the scope of the ordinary mould maker in South Africa who operates independently from the plastic product manufacturers. A need therefore exists to develop an affordable package that operates separately from the injection moulding machines. To be able to make the program available to the majority of mould makers it will have to be written for a personal computer.

INTRODUCTION

Polymer processing models are often phrased as field problems; a set of partial differential equations which govern the movement of the molten plastic and its accompanying heat transfer must be solved to find the values of the field variables within a spatial domain. Three equations need be solved simultaneously namely the continuity equation that describes the conservation of mass, the momentum conservation equation as well as the energy conservation equation. Solving the equations numerically requires a descritization process to convert the partial differential equations into a set of algebraic equations. These equations are then solved using the techniques of linear algebra and provide the field variable values at discrete points within the domain. There are three approaches, finite element, finite-difference and boundary element techniques, that can be followed in solving the governing equations.

The other important branch of the numerical simulation of polymer processing involves the realistic modelling of the polymer melt viscosity or more commonly known as polymer flow dynamics. An evident characteristic exhibited by the shear viscosity of polymer melts is a shear thinning behaviour with increasing shear rate. In addition to this the viscosity of polymer materials can also be highly dependant upon temperature and pressure as well. Since the injection moulding process is highly non-isothermal and can also involve significant pressure variations, it seems reasonable to expect that the temperature and pressure dependence of the melt viscosity will also be an important factor in the modelling of the injection moulding of thermoplastics.

During the filling stage of the injection moulding process the movement is caused by the presence of pressure gradients along the mould. The molten plastic comes into contact with the cooler walls and adheres to the walls with the result that there exists a velocity gradient perpendicular to the wall ensuring high shear stress flow. Due to the high viscosities of molten polymers the flow always has low Reynolds numbers resulting in laminar flow. Due to the low Reynolds numbers the inertial terms of the Navier-Stokes equations are negligible in comparison with the viscous terms. Body forces are

assumed negligible and together with the thin gap approximation the equations can be simplified with the Hele-Shaw approximation. The time dependant terms in the momentum equations are neglected due to the relatively long duration of the flow.

1.2 Literature survey

Firstly a quick overview of the main two classes of numerical methods used in plastic injection moulding simulation will be given after which previous work will be discussed.

1.2.1 Finite-difference and finite volume methods

The finite-difference method is the oldest and easiest to learn and to use. Finite-difference methods originated in the 1930's for hand calculation and their use expanded rapidly with the development of digital computers. Despite their limitations traditional finite-difference techniques still represent the most developed and best understood numerical procedure for solving partial differential equations. They also form the basis of more contemporary finite-difference methods namely the finite control volume methods which can handle a wide variety of complex problems.

A finite-difference solution to a field problem involves three steps. First, a grid is constructed over the problem domain. The grid represents the geometry of the domain and provides the discrete points where the solution will be computed. The discrete points, or nodes, are customarily identified as the intersections of grid lines and the dependant variables are computed at some point relative to these. The mesh can conform with rectangular Cartesian, cylindrical, or spherical coordinate systems, the choice being based primarily on the shape of the physical domain. An advancement on this method uses a numerically generated grid based on a non-orthogonal curvilinear coordinate system.

Once the grid has been constructed, the governing PDE's must be expressed in discrete form. This formulation or discretization step produces a set of finite-difference equations, which are algebraic expressions for the dependant variable values of the problem. Finally the algebraic equations must be solved numerically. Several methods are well-suited to the structure of finite-difference equations, the choice among them depends on the nature of the equations, computational efficiency, and the ease of programming. Numerical grid generation methods include both the creation of non-orthogonal curvilinear grids and the formulation of finite-difference equations on those grids. Traditional finite-difference methods lack the ability to model complicated shapes, but with non-orthogonal boundary fitted grids and numerical grid generation more complex geometries can be handled. Finite-difference methods with non-orthogonal boundary fitted grids can handle more complex shapes, but the methods are still not as powerful as finite element methods in respect of their geometrical modelling capabilities. Finite volume techniques which can be viewed as an extension of finite-difference methods approach the geometrical capabilities of finite element methods. Non-orthogonal boundary fitted grids with numerical grid generation makes finite-difference and finite volume techniques comparable to finite element methods in terms of geometric flexibility while retaining the simplistic character of finite-differencing.

The control volume approach derives finite-difference equations not by discretising the governing PDE's but by applying conservation principles directly to a macroscopic control volume. The control volume (CV) is chosen such that it forms a little box around a node with the nodal value representing the value over the entire control volume. For any scalar specific property ϕ related to fluid motion the conservation principle is written as follows

Net flux of ϕ into CV by convection + net flux of ϕ into CV by diffusion + generation of ϕ in the CV = increase of ϕ in CV

Convection into the control volume takes place due to the motion of the fluid. The diffusive flux is usually linearly related to the gradient of the property by a diffusion coefficient. To evaluate any variable on a CV boundary, linear interpolation or the arithmetic mean of the values at the adjacent cells are used. For accuracy it is important that the differential equation be in the conservative form so that the flux of ϕ across the face of the control volume should be the same for both of the volumes sharing the same face. Conservative forms satisfy the conservation principles locally as well as globally which leads to a more accurate and stable solution.

The practical value of the control volume approach lies in analysing domains with complex geometries which require irregular node spacing. Conservation principles can be applied to each volume to obtain a set of algebraic equations containing the unknown values of the problem variables within each control volume. An analysis of this type requires careful manipulation of the variables at the volume boundaries. In the case of mould filling applications, additional bookkeeping becomes necessary to track the location of the advancing polymer front. The control volume approach generates economical solutions and can be applied to complex geometries with relative ease.

1.2.2 Finite element methods

The finite element method originated in the 1960's as a technique for structural analysis. Since that time, and in parallel with the advances in computing power that have occurred, it has now developed into a powerful technique for the solution of a wide range of differential equations arising in engineering and science.

A major advantage of the method is its geometrical flexibility. It is easy to carry out solutions on domains of irregular shape and to vary resolution within the solution domain to concentrate computing effort where it is needed. Boundary conditions are treated in a convenient way, especially those involving flux or derivative conditions. Additionally information defining the geometry and boundary conditions is handled as input data, so that the program may be applied without alteration to an indefinite number of problems. Another big advantage which the finite element method has over other methods is that smooth variations in property values can be interpolated within elements.

Modelling hot thermoplastic processes with the finite element method requires that many of the most difficult aspects of the finite element method be addressed in the analysis. These difficulties arise because of large strains, large deformations, nonlinear material behaviour, contact between polymer and the mould wall and the advancement of the moving front. All these complications lead to a set of non-linear equations which have to be solved in an iterative manner. Due to the equations being solved in an iterative manner many of its advantages in terms of computational efficiency is lost to its main rival the finite volume method.

In the finite element method, a body to be analyzed is divided into a number of small subdivisions, or finite elements. The elements are defined by a number of nodal points, which for the elements considered are their corner points. For cavities of complex plastic parts, triangular elements are preferred to quadrilateral elements for the following reasons;

* Highly irregular shapes can be more easily divided into triangles than into quadrilaterals
* For the same number of nodes, triangular elements provide greater flexibility than quadrilateral elements in distributing nodes inside the calculation domain.

The variational finite element formulation involves the minimization of the integral of the PDE over the flow field of the appropriate functional in which derivative boundary conditions are included. This part of the procedure is called the variational formulation of the problem and can be compared to the writing of the governing equation in an algebraic form of the finite-difference method. The displacements of the node points are unknowns in the finite element analysis. Inside an element, the displacements are interpolated between the nodes of the element using a polynomial interpolation function. In plastic modelling it is usually assumed that these displacements vary linearly along the edges because the polymer can be severely deformed when it comes into contact with the mould wall resulting in abrupt changes. Elements with a higher order interpolation function can be overly deformed when subjected to these conditions and this gives rise to numerical instabilities.

The finite element method requires plenty of memory during computations because interpolation functions need to be defined and stored for each element. This also adds to finite element methods being slower in execution especially when non linear problems are solved that require an iterative approach. Most commercial plastic injection mould simulation codes model the polymer process with the finite element method. These packages also only run on work stations, are linked with CAD/CAM/CAE interfaces, and are very costly indeed.

1.2.3 Previous work

A number of studies have been proposed for the simulation of injection moulding processes with varying degrees of complexity, depending on the mathematical formulation of the flow equations, other assumptions relating to material properties, and the treatment of the resulting set of equations.

In the early fifties serious research work on injection moulding started with the work of Spencer and Gilmore(1949). They were the first to describe the fluid dynamics and the pressure drop during mould

filling as well as to consider the problems of orientation and internal stresses. They employed an empirical equation for capillary flow and coupled it with a quasi steady-state approximation to calculate the filling time. Since then different models have been proposed to describe the moulding cycle. During the sixties and seventies the research trend was to analyze simple one-dimensional flow behaviour in rectangular and centre-gated disk shaped thin cavities. At the same time researchers investigated one-dimensional non-isothermal flow in circular and non-circular tubes. During the early eighties the research trend was to investigate the flow in thin cavities of arbitrary planar geometry based on the Hele-Shaw type of flow. Concerning the practical application to more complex geometries, two approaches have been proposed, namely the flow analysis network (FAN) method (Broyer, Gutfinger & Tadmore, 1975) and the branching flow method (Wang, Hieber and Wang, 1986).

The (FAN) method uses a "lay flat" procedure to decompose the three dimensional cavity geometry into one-dimensional flow paths, each of which consists of a series of simple one-dimensional flow segments. (strips, disks or tubes) A one-dimensional flow analysis is then applied to each of the flow paths which are then coupled by requiring that the total pressure drop be the same along each flow path subject to the constraint that the total flow rate be satisfied. The branching flow method calculates the melt front pattern relative to a mesh configuration consisting of rectangular elements. Special treatment is required at the boundary conditions at the border nodes since the underlying rectangular elements cannot fit exactly into an arbitrary shape.

Reported in various articles published during the mid eighties Wang and Hieber (1988) together with co-authors from Cornell University did pioneering research work into the field of injection moulding simulation and currently market a commercial code called C-Flow. They combined the finite element formulation for the pressure equation with the finite-difference formulation for the energy equation

to solve generalized Hele-Shaw flow with the FAN approach that was mentioned earlier. A form of the control volume scheme was used that handles automatic melt-front advancement in practical three dimensional geometries. At the same time other researchers used the Marker and Cell (MAC) finite-difference technique to follow the free boundary of the advancing melt (Harlow and Welch, 1965). This method involves the spreading of marker particles all over fluid occupied regions with each particle specified to move with the fluid velocity at its location. The newest method of tracing the melt front advancement is by means of the Volume of Fluid method (VOF) (Hirt and Nichols, 1981). This method assigns a pseud-concentration throughout the mesh in such a manner that its value indicates the presence or absence of fluid. It is assumed that the concentration is transported by convection alone and hence an extra equation needs to be solved. In all cases the filling stage is limited to purely viscous fluids of constant densities. The reader has now been exposed to a broad outline concerning the development of numerical simulation in plastic injection mould design. Individual articles and publications will now be investigated.

Broyer, Gutfinger & Tadmore (1975) did pioneering work when they extended the flow analysis network (FAN) method, previously developed for die design, to the problem of the cavity filling process in injection moulding. Under the assumption of Hele-Shaw type flow in narrow passages they performed a complete analysis of the injection moulding process by means of the finite element method. To model the free front using the (FAN) method they describe the geometry in terms of a fixed grid and scalar parameter, ϕ, for each rectangular cell. The parameter ϕ gives the ratio of the occupied to the total volume of each cell. The mould is divided into equal square elements with the assumption that the fluid in each element is concentrated at the centre, or node, of the square. The nodes of adjacent squares are linked together and from the conservation of mass principle the nett outflow from a field node should be zero. From this the pressure field is calculated and they update

the corresponding values of ϕ for an elapsed time increment. They were also the first to simulate a non-Newtonian fluid in plastic injection moulding.

Kamal and Lafleur (1982) in a very theoretical article reviewed previous work by Hieber and Shen (1980) who employed the generalized Hele-Shaw flow for the modelling of the filling process by means of a finite element numerical technique. They claim that the application of fully developed Hele-Shaw flow gives rise to errors in the entrance region and is also unsatisfactory in the representation of the front region. In an attempt by them to develop a model to represent the entry and fully developed regions, some assumptions which are less restrictive than for the Hele-Shaw flow are made. The equations of mass, momentum and energy for the case of a non-Newtonian fluid flowing in a thin, rectangular cavity are simplified as a result of the following assumptions:

* The fluid motion is laminar
* Body forces are negligible
* The unsteady-state terms in the momentum and continuity equations are neglected in view of the comparatively long duration of the flow
* There is no velocity component in the z direction (except near the front)
* Viscous forces are considerably greater than inertia forces

They state that any more assumptions on the equations of flow would lower the quality and utility of the solution and would lead to Hele-Shaw flow. Their set of equations still retains the pressure gradient in the gap width direction.

Lafleur and Kamal (1986) describe the simulation of the mouldability parameters of the injection moulding process, namely the pressure drop in the delivery system and the melt front progression during cavity filling among other phenomena. All this is done with a new mathematical model which they propose and verify experimentally in part two of the same article. The analysis is restricted to

two dimensional motion in a plane resulting in the hydrodynamic and energy equations being developed for a two dimensional Cartesian co-ordinate system. The authors do not use the Hele-Shaw flow approximation and solve the Navier-Stokes equations with the following simplifying assumptions for the filling stage.

* The fluid is assumed to be viscoelastic and incompressible
* The body forces are negligible.
* Gradients in the gap wise direction are negligible leading to two dimensional flow (They are simulating a rectangular mould in two dimensional Cartesian co-ordinates)
* The terms involving pressure in the energy equation are neglected.

They utilise a finite-difference numerical scheme and defend this by saying that the wall boundaries are straight making this scheme simple and straightforward in principle. They express the equations in a finite-difference form using central difference formulae in a semi-implicit way because all the non-linear terms in the momentum and stress equations are written in explicit form. They also use the Marker-and-Cell method in solving the free surface. After the simulated results were compared to the experimental results they conclude that the predictions of pressure variation with time are excellent at the entrance and reasonably good at the centre of the cavity. They justify this by mentioning that the melt front positions did not correlate and this could be the reason for the pressures being different.

Couniot, Dheur, Hansen & Dupret (1988) presented a paper which is devoted to the non-isothermal simulation of the filling of thin planar or three dimensional parts using the Hele-Shaw flow approximation. What makes their contribution unique is that at any time step during the filling stage, approximate pressure and temperature fields are calculated using successive finite element meshes, which are generated on the filled part of the mid surface. They use a Lagrangian flow model in describing the moving front. The remising algorithm is very complex and is not discussed. Fountain flow effect is addressed in detail in this paper. Fountain effect occurs due to the main viscous flow

being parallel to the mid surface, resulting in the velocities being deflected towards the walls in the front region. This effects the temperature distribution at the free front and hence weld line formation. A few examples are presented in detail and the authors conclusion is that the algorithm appears to be relevant.

Wang and Hieber (1988) report on advances made to the modelling of the cavity filling stage in terms of a melt viscosity which depends upon shear rate, temperature and pressure. They emphasize that simulation is heavily dependant upon a realistic modelling of the polymer melt viscosity, because the filling corresponds to creeping, shear dominated flow which is treated in terms of classical Hele-Shaw flow generalized to a non-Newtonian, non-isothermal, non-steady flow problem. It is also assumed that viscoelastic effects are not important and support this with experimental validation. This indicates that inelastic modelling can quite adequately predict the shape of the advancing melt front in the cavity as well as the attendant pressure field. A finite element/finite-difference procedure was developed for solving the problem, using triangular elements with quadratic shape functions for pressure and linear shape functions for temperature. Time dependant nodal pressures are stored at each vertex and mid side node whereas the time dependant gapwise temperature profiles are stored at every vertex node with the gapwise distribution being represented in terms of a finite-difference mesh across the half gap thickness. The authors employ a new development for the advancement of the melt front. Where the old method was to use a predictor corrector scheme, they employ a fixed finite element grid and use a control volume approach which makes the melt front advancement amendable to an automated algorithm. They also state that the five constant material model is adequate for the filling stage and that the seven constant model need only be used in the post filling stage. All their theories are supported with experimental verification.

Kamal, Goyal & Chu (1988) present a detailed two dimensional mathematical model of injection mould filling in a rectangular cavity that takes into account the effect of the slip boundary condition in obtaining a realistic simulation of fountain flow. In the case of thin cavities found in plastic injection moulded products, the variations in the gap wise or width direction are neglected. Hence they solve the two dimensional Navier-Stokes equations on a rectangular grid. They mention that many previous researchers have not incorporated the slip boundary into the mathematical modelling of injection mould filling. They explain that a dynamic three phase contact line exists where the interface between liquid and a second immiscible fluid intersects the solid surface, and the movement of contact lines violates the adherence, or no-slip boundary condition that is otherwise obeyed by all flowing fluids. Special consideration is thus given to the shape of the flow front. In the non-isothermal case the model considers the moving boundary due to solidification of the polymer melt next to the mould walls. The flow equations, which are not simplified using Hele-Shaw flow, were solved using a finite-difference technique with the Marker-and-Cell method used to track the advancing melt front. A rectangular mould was used and the results compared to experimental results. They conclude that it is necessary to use a slip boundary condition to maintain an accurate shape of the flow front.

Narazaki and Mizukami (1990) explain the development of a finite element code "MOLDIA-F" and present some numerical examples. They use the classical Hele-Shaw approximation of the flow equations together with a modified four constant material model. What distinguishes their contribution is that they use the Volume-of-Fluid (VOF) method in tracing the advancing melt front. They conclude by saying that the formation of weld lines is of great concern to the appearance and strength of a plastic product and that it should be very helpful that we can predict the formation of the weld lines on a computer.

1.2.4 Conclusion of the literature survey

An extensive literature survey indicates that the thin gap numerical model, using the Hele-Shaw formulation of the governing equations, is the most efficient for the simulation of plastic flows. The literature survey also shows that most packages using the thin gap numerical model utilise the finite element method in solving the non-linear equations. The most modern method of tracking the free front is to use the Volume-of-Fluid approach which was developed by Hirt and Nichols (1981). Most of the commercial packages available use the finite element method which is known to be slower in execution and more memory intensive than the finite volume method. These packages operate on expensive work stations using the UNIX operating system and is beyond the financial constraints of the ordinary mould maker in South Africa.

1.3 Aim of the study

The main objective of the study is to develop a thin gap numerical model using the Hele-Shaw formulation of the Navier Stokes equations for the filling stage of the injection moulding process. An extensive literature survey indicates that the thin gap numerical model is the most efficient for the simulation of plastic flows and will be the most applicable model for achieving the other objectives. It was decided to follow the finite volume approach because indications are that it will be faster than the finite element method, a consideration which is very important when implementing the method on a personal computer. Another reason why the finite volume method was chosen is because of the existing expertise in the research group in which the author worked.

Due to molten plastic being a non-Newtonian fluid the viscosity is dependant on the flow variables that are being solved. An applicable and reliable material model needs to be implemented that will ensure that the simulated results are realistic. An algorithm for tracking the free front also needs to be incorporated into the model.

The objectives of this study are summarized as follows:

i) To describe the development of a thin gap numerical model utilising the Hele-Shaw formulation of the Navier-Stokes equations for the simulation of the filling stage of the injection moulding process.

ii) To develop a program that can be implemented on any IBM-compatible personal computer that will fall within the budget of the ordinary mould maker.

iii) To implement an applicable material model.

iv) To develop an algorithm that simulates the movement of the free front during the filling process.

1.4 Overview of the study

After the introduction into the field Chapter 2 deals with the basic computational model and decisions as to which methods will be used, are taken and justified. The governing equations for the fluid flow are described and descritised using the control volume approach. The relevant boundary conditions are described and non-viscous isothermal simulations performed. Finally the chapter is concluded with numerical experiments that test the model against theoretical predictions.

Chapter 3 expands the model to include the movement of the free surface. References are made to the literature survey and a method is selected. The method is implemented and tested. The diffusive nature of the equation is explained and an algorithm to smooth it is also proposed. The effect of the time step on the moving boundary is investigated in terms of the Courant number and the way in which it alters the existing program is also explained. Finally the material model is incorporated.

Chapter 4 explains the development of the code to allow it to model thin three dimensional parts. The model is based on three-dimensional shell volumes and the derivation of the transformation of the flow equations to general coordinates are explained in detail.

The thesis is concluded in Chapter 5 with a summary of the whole study and recommendations for further research into this field.

2 COMPUTATIONAL MODEL

2.1 Introduction

In this chapter the governing equations of fluid flow are presented along with the simplifications required for the Hele-Shaw formulation. Reasons are given as to why the Hele-Shaw formulation is chosen above the other more comprehensive formulations. The finite volume/finite-element discussion is attended to again as to why the finite volume method was chosen.

The Hele-Shaw flow equations are then discretized on a rectangular Cartesian domain and implemented. Continuous flow through a flat rectangular cavity with a high aspect ratio, representing a mould for a typical thin-walled product is considered. The flow at first is an isothermal Newtonian flow with a constant viscosity. With this flow we can compare the model against analytical results. The relevant boundary conditions are discussed in detail.

A rectangular domain is then introduced where the melt gets injected at a corner and tests are performed which check for symmetry, before the free front gets implemented into the code which is dealt with in the next chapter.

2.2 Governing equation approximations

Generally speaking, viscous fluid flows are governed by the Navier-Stokes equations. But injection mould cavities are often narrow in one dimension, and the high viscosity of polymer melts makes inertia effects negligible in comparison to viscous effects in injection mould filling. This enables us to simplify the Navier-Stokes equations. The reason why we want to simplify the equations is that the discretization is easier, the solution algorithms are less complicated, converge easier, quicker and use less memory. By not simplifying the governing equations, the simulation is made more costly in terms of computer power and speed which does not contribute to the overall accuracy of the solution.

Since the inertia forces are proportional to the square of the velocity whereas the viscous forces are only proportional to its first power, it is easy to appreciate that a flow for which viscous forces are dominant is obtained when the velocity is small, or more generally when the Reynolds number is small. Molten plastic has a very high viscosity and a relatively slow velocity which ensures a very low Reynolds number. This allows us to simplify the Navier Stokes equations into the three-dimensional equations of creeping motion, Schligting (1979). The Hele-Shaw approximation is essentially a solution of the three dimensional equations of creeping motion that are presented in Schligting (1979) for the viscous motion of flow between two parallel flat walls that are separated by a small distance 2h.

The literature survey indicates that the generalized Hele-Shaw (GHS) formulation has become the standard way to formulate injection mould filling processes. The method is fast and simple but a disadvantage of the method is that it is inaccurate in the entrance and front regions. It is not known from the literature survey to what extent the Hele-Shaw formulation loses in accuracy to the more advanced formulations. Although the more advanced formulations will be more accurate in the mentioned regions, these regions constitute only a small portion of the overall geometry. It is doubtful if these more advanced formulations will have a significant effect on the accuracy of the overall results. Our aim is to develop an inexpensive commercial package that runs on a personal computer which provides useful results. The Hele-Shaw approximation is suitable in achieving these goals.

2.3 Finite element versus finite-difference approaches

The literature survey indicates that both the finite element and finite difference techniques have been employed in numerical schemes simulating the polymer melt flow. Most of the articles indicate that the finite element method is more popular among researchers than the finite difference/finite volume techniques are. A possible reason for this is that the finite element methods deal with irregular geometries easier than other methods do. What was apparent in the literature survey was that the

finite volume/finite difference methods were only applied to rectangular cavities in Cartesian coordinates for research purposes. The stream function vorticity formulation of the Hele-Shaw equations was also solved with finite difference methods.

The latest developments in Computational Fluid Dynamics (CFD) have shown that the finite volume approach is a very powerful method in simulating fluid flow problems. These developments include unstructured grids which make finite volume methods as powerful as finite element methods in simulating flow problems with very complex geometries. The literature survey shows that these developments have not yet been applied to polymer melt flow.

It has been reported in Chapter 1 that finite volume methods are easier to use than finite element methods. This is due to the uncomplicated conservation principles that are applied to the control volume, whereas the finite element method requires interpolation functions over elements to describe the dependant variables. The order of these interpolation functions can make the finite element solution more accurate than the finite volume method. It was also reported in the literature survey that due to the viscous and non-linear nature of the hot plastic melt the most difficult aspects of the finite element method needs to be addressed when modelling the plastics injection moulding process. This requires that the interpolation functions must be linear otherwise numerical instabilities occur, which makes it as accurate as the finite volume method is in this respect. Due to the non-linear nature of the plastic the finite element algorithm is iterative in nature which tends to slow down the solution. The finite volume method is also an iterative method but it requires less computational effort per iteration which makes it faster than the finite element method. Therefore, due to the simplistic nature of the control volume methods, they are generally faster than finite element methods are for convection diffusion phenomena. This is a very important point when developing a model that will run on a personal computer.

Almost all the commercial packages that use the Hele-Shaw formulation to simulate polymer melt flow employ a finite element method or a hybrid finite element/finite difference method. There is yet no package that uses the latest finite volume techniques to simulate the filling stage of the injection moulding process. Due to the advantages that these methods have in terms of memory and speed, they hold promise for developing an inexpensive commercial package that operates on a personal computer.

2.4 Governing equations

We consider a thin cavity in a solid mould as shown in Figure 2.1 with the coordinate system as shown. Here the molten plastic flows in the x and y directions and the z direction is perpendicular to the mean velocities. The x-y plane in the real geometry may be a curved surface which lies on the middle of the two solid boundaries, but if the gap of the two boundaries is sufficiently small as compared with the radius of curvature, this surface can be flattened into a plane for the purpose of the analysis.

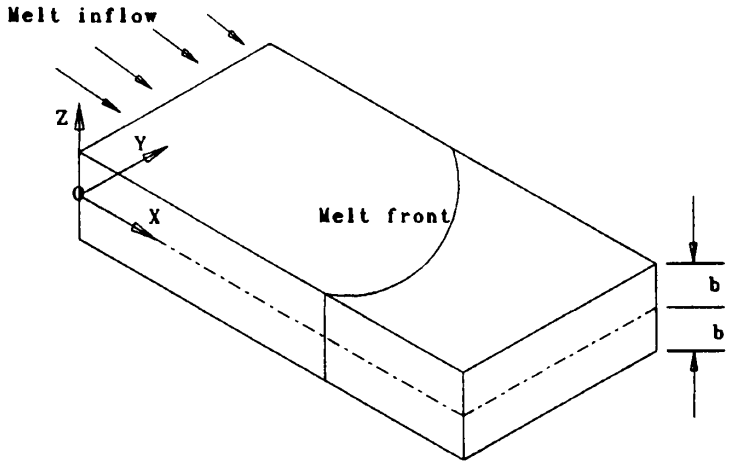

Figure 2.1. Thin cavity indicating the origin and gap.

The solid boundaries are denoted by

$$z = \pm b(x,y) \tag{2.1}$$

where b is the half gap, and the no slip boundary condition is applied to the velocity there.
The transport equations governing the motion of any viscous fluid are the Navier Stokes equations. These equations are simplified, using the Hele-Shaw approximation which, according to Schlichting (1979), is very appropriate for highly viscous fluids flowing through thin gaps. The Hele-Shaw approach is based on the following simplifying assumptions:

* The velocity component in the z direction is neglected and pressure is a function of x and y only.
* The inertial terms are negligible in comparison with the viscous terms.

Applying the Hele-Shaw approximation to the x-momentum equation results in

$$\frac{\partial p}{\partial x} = \frac{\partial}{\partial z}\left(\eta \frac{\partial u}{\partial z}\right) \tag{2.2}.$$

The momentum equation in the y direction becomes

$$\frac{\partial p}{\partial y} = \frac{\partial}{\partial z}\left(\eta \frac{\partial v}{\partial z}\right) \tag{2.3}.$$

and in the z direction we have

$$\frac{\partial p}{\partial z} = 0 \tag{2.4}.$$

For an incompressible fluid the continuity equation can be written as

$$\frac{\partial u}{\partial x} + \frac{\partial v}{\partial y} = 0 \qquad (2.5).$$

The thickness averaged continuity equation, is given by

$$\frac{\partial (b\bar{u})}{\partial x} + \frac{\partial (b\bar{v})}{\partial y} = 0 \qquad (2.6)$$

where b is the half gap thickness and the overbar - denotes an average over z.

With the energy equation thermal conduction in the direction of the flow and thermal convection in the thickness direction is neglected, based on the thin gap approximation (Hieber & Shen, 1980), giving

$$\rho C_p \left(\frac{\partial T}{\partial t} + u\frac{\partial T}{\partial x} + v\frac{\partial T}{\partial y} \right) = \kappa \frac{\partial^2 T}{\partial z^2} + \eta \dot{\gamma}^2 \qquad (2.7).$$

It should be noted that the velocities in the convection term can be approximated by their gapwise average values giving

$$\rho C_p \left(\frac{\partial T}{\partial t} + \bar{u}\frac{\partial T}{\partial x} + \bar{v}\frac{\partial T}{\partial y} \right) = \kappa \frac{\partial^2 T}{\partial z^2} + \eta \dot{\gamma}^2 \qquad (2.8).$$

The shear rate is given by (Narazaki and Mizukami, 1990):

$$\left.\begin{aligned} \dot{\gamma} &= \sqrt{\left(\frac{\partial u}{\partial z}\right)^2 + \left(\frac{\partial v}{\partial z}\right)^2} \quad or \\ \dot{\gamma} &= \left(\frac{z}{\eta}\right)\sqrt{\left(\frac{\partial p}{\partial x}\right)^2 + \left(\frac{\partial p}{\partial y}\right)^2} \end{aligned}\right\} \qquad (2.9).$$

Since p is independent of z (see Eq 2.4) and the velocity can be assumed to be symmetric with respect to z, Equations (2.2) and (2.3) can be integrated to give

$$z\frac{\partial p}{\partial x} = \eta\frac{\partial u}{\partial z} \qquad (2.10)$$

and

$$z\frac{\partial p}{\partial y} = \eta\frac{\partial v}{\partial z} \qquad (2.11).$$

Another integration of Equations (2.10) and (2.11) yields

$$u = \int_0^z \frac{\partial p}{\partial x}\cdot\frac{\xi}{\eta}\cdot d\xi + u_o \qquad (2.12)$$

$$v = \int_0^z \frac{\partial p}{\partial y}\cdot\frac{\xi}{\eta}\cdot d\xi + v_o \qquad (2.13)$$

where the subscript o denotes the velocities on the centre line. These two equations give the velocity profiles in the gapwise directions. The classical Hele-Shaw method only deals with the average velocities in the gapwise directions and hence Equations (2.12) and (2.13) become

$$S\frac{\partial p}{\partial x} = -b\bar{u} \tag{2.14}$$

$$S\frac{\partial p}{\partial y} = -b\bar{v} \tag{2.15}$$

where S is given by De Kock (1993)

$$S = \int_0^b \frac{z^2 dz}{\eta} \tag{2.16}.$$

with the average velocities given by

$$\left.\begin{aligned} b\bar{u} &= \int_0^b u\ dz \\ b\bar{v} &= \int_0^b v\ dz \end{aligned}\right\} \tag{2.17}.$$

Substituting Equations (2.14) and (2.15) into Equation (2.3) results in the governing differential equation for pressure for the Hele-Shaw flow approximation.

$$\frac{\partial}{\partial x}\left(S\frac{\partial p}{\partial x}\right) + \frac{\partial}{\partial y}\left(S\frac{\partial p}{\partial y}\right) = 0 \tag{2.18}.$$

In conclusion, the primary governing equations are (2.7) and (2.18) for temperature and pressure respectively. The classical Hele-Shaw formulation uses the approximate Equation (2.8) as the energy equation. When this equation is used only the average velocities are stored for the gapwise direction instead of the velocity profile and hence memory is saved. Equations (2.12) and (2.13), which calculate the velocity profiles, need not be programmed resulting in a quicker execution time. The average velocities are always calculated because they are required for most front tracking algorithms. The energy equation, Eq. (2.8), is written in conservative form before it is discretized, enabling the convection terms to be written in terms of volumetric flow rate fluxes which are calculated from the two-dimensional pressure gradients. It is only in the energy equation where the actual profile can be used so the accuracy of the overall method should not be affected too much when using the average velocities. The related variables are calculated directly from the other equations that are given.

2.5 Discretization of the governing equations

When developing a model to simulate a dynamic process it is usually conceived on a very simple domain with very elementary boundary conditions. If the program gives accurate solutions on an uncomplicated grid then the solutions should be realistic on a more advanced grid as well. At first not all the governing equations are solved at once either. The program is developed in stages. By doing it this way the programmer can debug the program more efficiently and perform meaningful experiments in validating the results.

For the development of the basic model a rectangular mould as shown in Figure 2.2 was chosen for the initial simulations. First a two dimensional orthogonal computational grid is constructed over the calculation domain. The domain is then divided into a number of non-overlapping control volumes in such a way that each grid point, except those on the domain boundary, is surrounded by one control volume. This arrangement of control volumes requires the spacing between the nodes at the boundaries to be half the spacing elsewhere, provided the grid has equally spaced nodes, as is shown

in Figure 2.2. The solid lines indicate the mould and the dotted lines the computational grid. Typical control volumes are shown (Figure 2.2) on the boundary, in the corner and on the domain itself.

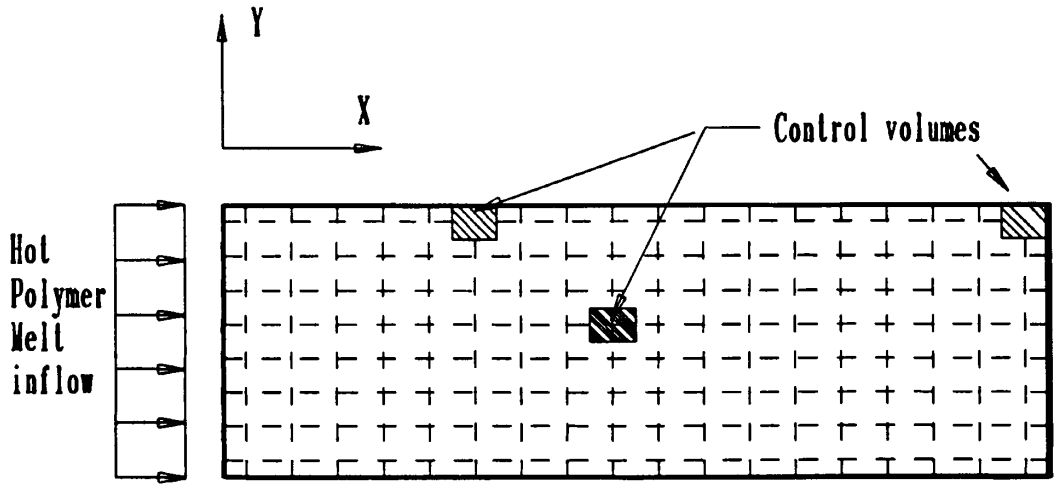

Figure 2.2. Mould indicating the computational domain and the control volumes.

2.5.1 Pressure equation

The partial differential equation governing the pressure Equation (2.18) is discretized using a grid system in the x-y plane as depicted in Figure 2.3. In this figure, P depicts the node at which an unknown variable is to be computed. An integrational cell or control volume is identified by the dotted lines. The central idea behind the control volume approach is to relate the values at the computational nodes P to the values of the variables at the neighbouring nodes N,S,W,E,NE,NW,SE,SW. The set of equations so constructed are solved simultaneously to give values for the unknowns in each control volume in the domain. For each control volume the general discretized form of the governing equation gives the relation between the dependant variable ϕ at the cell centre P, and the neighbouring values of ϕ as follows:

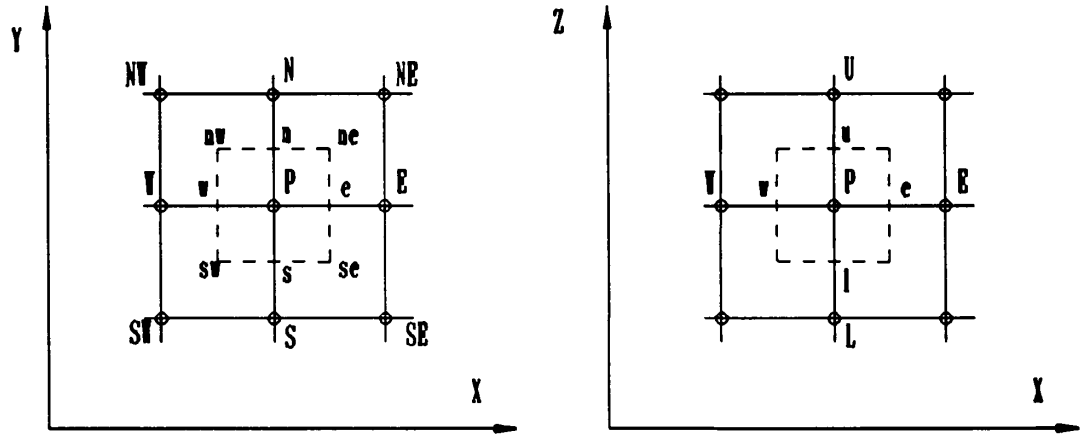

Figure 2.3. Notation for discretization of equations using control volumes.

$$(A_p + A_t)\phi_P^t = \sum A_{nb}\phi_{nb} + B + A_t\phi_P^{t-1} \qquad (2.19)$$

where A_{nb} are the neighbouring coefficients, ϕ_{nb} are the neighbouring ϕ values and $(S + A_t\phi^{t-1})$ is the source term.

Equation (2.18) was descritised using finite volume formulations according to the notation given in Figure 2.3 and Equation (2.19) where ϕ = p, the pressure. In a Cartesian grid the finite volume and finite difference formulations give the same results. With a finite difference method, differences are

taken across the grid whereas with a finite volume method the equation is integrated over the control volume. The resulting coefficients are:

$$\left.\begin{aligned} A_E &= \left(\frac{S_e \Delta y}{\Delta x_e}\right) \\ A_W &= \left(\frac{S_w \Delta y}{\Delta x_w}\right) \\ A_N &= \left(\frac{S_n \Delta x}{\Delta y_n}\right) \\ A_S &= \left(\frac{S_s \Delta x}{\Delta y_s}\right) \end{aligned}\right\} \qquad (2.20)$$

The coefficient A_P is the sum of the neighbouring coefficients. Therefore

$$A_P = A_N + A_S + A_E + A_W \qquad (2.21).$$

The final descritised pressure equation is given by:

$$A_P p_P = A_E p_E + A_W p_W + A_N p_N + A_S p_S + B \qquad (2.22).$$

The source term B in the above equation is the volume source. If no fluid volume is injected into a cell (finite volume) the source term will be zero. With injection moulding the fluid is injected into the mould at a constant flow rate of q[m^3/s]. In order to model this we need to place a source term at the nodes where the fluid is being injected into the mould. The inflow boundary can also be dealt with by specifying the pressure gradient at the inflow boundary. Specifying a pressure gradient at the inlet is equivalent to specifying an inlet velocity. The source approach has to be used when one injects into the interior and for our objectives this approach is sufficient. Hence at the nodes where molten plastic is being injected, the source term is given by

$$\boldsymbol{B} = \boldsymbol{q} \tag{2.23}$$

2.5.2 Volumetric flow rate fluxes

It was mentioned in Chapter 1 that from the viewpoint of accuracy it is important that the differential equation be in conservative form. This means that the transport equations are written in such a way that the convective terms partial differential equations have no coefficients. The transport equations can easily be written in conservative form because the continuity equation must always be satisfied (Anderson, Tannerhill and Pletcher, 1984). Conservative forms satisfy the conservation principles locally as well as globally which leads to a more accurate and stable solution. When an equation is discretized in conservative form then the flux of a scalar quantity ϕ across the face of the control volume should be the same for both volumes sharing the same face.

For the above mentioned reasons the equations with convective terms are first written in conservative form and then discretized. The volumetric flow rate fluxes on the volume faces are then required. These fluxes are now defined and stored globally in the program because they are used for more than one equation. When one works with the flux method it is easy to check if continuity is satisfied in a specific volume and this is important when the front tracking algorithm is incorporated. So all the equations involving convective terms are expressed in terms of fluxes. The fluxes are derived from the thickness averaged continuity Equation (2.3). This equation is then integrated in the same way as Equation (2.18) across the control volume (Figure 2.2) ensuring that both the pressures and fluxes are compatible with each other. The resulting fluxes are

$$\left.\begin{aligned} F_e &= S_e\left(\frac{p_E - p_P}{\Delta x_e}\right)\Delta y \\ F_w &= S_w\left(\frac{p_P - p_W}{\Delta x_w}\right)\Delta y \\ F_n &= S_n\left(\frac{p_N - p_P}{\Delta y_n}\right)\Delta x \\ F_s &= S_s\left(\frac{p_P - p_S}{\Delta y_s}\right)\Delta x \end{aligned}\right\} \qquad (2.24).$$

Only two flux values, i.e. north and east, need be stored per control volume because the flux values are the same for neighbouring volumes sharing the same face. The sum of all the fluxes in Equation (2.24) should be zero if continuity is satisfied. By working with fluxes instead of velocities the chances of numerical round-off errors are reduced because the fluxes have a favourable order of magnitude.

2.5.3 Energy equation

In the energy Equation (2.7) thermal convection in the thickness direction and thermal conduction in the direction of flow is neglected. Central difference forms in the energy equation are only adequate when convection is small compared to conduction in the same direction and this does not occur in the present situation. This means that the results will be inaccurate or the solutions will become unstable if we use central differencing. The problem arises from the non-linear terms associated with the convection of energy where central differencing gives rise to the solution becoming unstable if the cell Reynolds number or Peclet number is larger than 2. One solution to this problem is to use

upwind differencing for the convective terms. Another solution is to use a hybrid formulation incorporating both central and upwind differencing or to describe the convèction with another function (Patankar, 1984).

The conduction terms in the equation are descritised using central difference formulations because these terms are diffusive in nature and a central difference algorithm will not cause instabilities in the solution. The energy equation in the Hele-Shaw flow formulation is also time dependant and for this we use an implicit formulation. An implicit formulation is unconditionally stable whereas an explicit formulation is only conditionally stable. The energy equation can be solved iteratively by specifying an infinite time step or transiently by specifying a finite time step.

Equation (2.8) was multiplied by the half gap width b and written in conservative form allowing it to be discretized, using upwind differencing, in terms of the fluxes defined in Equation (2.24). The energy equation is the only equation in the classical Hele-Shaw formulation that is three dimensional. The same notation detailed in Figure 2.3 was used for the x-y and the x-z planes in the discretization. The coefficients are then applied in the same form as given by Equation (2.19) where ϕ=T. The coefficients are:

$$\left.\begin{aligned} A_t &= \frac{\rho b C_p \Delta x \Delta y}{\Delta t} \\ A_E &= \max(0, -\rho C_p F_e) \\ A_W &= \max(0, \rho C_p F_w) \\ A_N &= \max(0, -\rho C_p F_n) \\ A_S &= \max(0, \rho C_p F_s) \\ A_U &= \frac{\kappa \Delta x \Delta y b}{\Delta z \Delta z_u} \\ A_L &= \frac{\kappa \Delta x \Delta y b}{\Delta z \Delta z_L} \\ B &= \eta \Delta x \Delta y \dot{\gamma}^2 b \end{aligned}\right\} \qquad (2.25)$$

2.5.4 Calculation of the quantity S

An integration quadrature formula is used to calculate S given by Equation (2.16). Figure 2.4 gives the notation for applying the following integration quadrature to Equation (2.16).

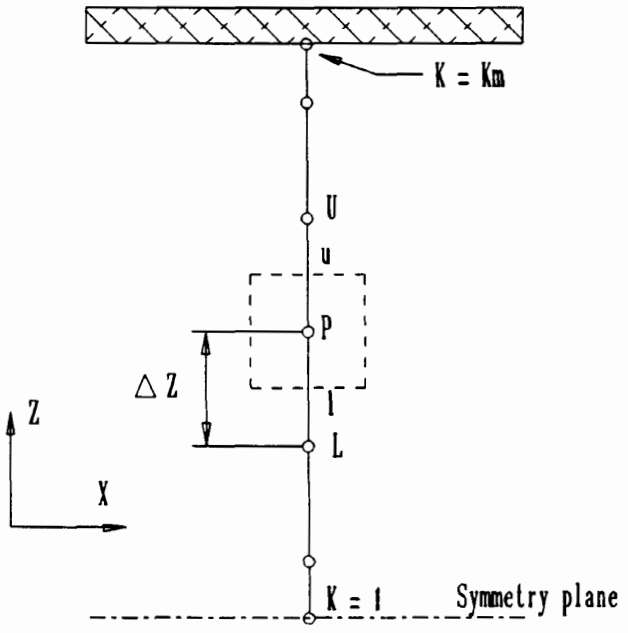

Figure 2.4. Notation used for the integration quadrature of S.

The value of S is a two dimensional quantity which is obtained from integrating or summing in the z gapwise direction:

$$S_P = S_L + \left(\frac{z^2}{\eta}\right)_l \cdot \Delta z \quad \text{where} \quad P = 2,\ldots,K_m \tag{2.26}$$

2.6 Boundary conditions

The governing equations have been defined and discretized in this chapter. In order to solve the system of equations, the variables must be defined at the boundaries. The type of boundary conditions depend on the type of boundary under consideration.

2.6.1 Pressure equation

At the gate or the inlet, either a constant flow rate or a pressure gradient needs to be specified. A pressure boundary condition can also be specified at the inlet for validating the numerical model. At positions on the mould where ventilation holes are specified a constant atmospheric pressure boundary condition is applied. Along the solid walls of the mould, i.e. walls in the x-z or y-z planes (Figure 2.1), a zero gradient boundary condition is used for the pressure equation, provided there are no ventilation holes in these walls.

2.6.2 Energy equation

With the thin gap numerical model we split the geometry along the plane of symmetry and consider only half the mould. The centre plane is a symmetry plane. The temperature profile has a zero gradient boundary condition along the symmetry plane. On the solid walls of the mould a no slip fixed boundary is applied. The temperatures are specified on all solid walls throughout the mould. The temperature at the inlet is the temperature of the hot molten plastic which enters the mould.

2.6.3 Initial conditions

Numerical solvers that solve problems arising from partial differential equations by iteration require initial conditions in addition to boundary conditions. These initial conditions need to be chosen cautiously when simulating plastic injection moulding processes. If the temperature equation were to be solved using an iterative solver the initial conditions would have to be specified in such a manner that the viscosities which are temperature dependant produce realistic results. The ideal initial condition in this case would be the temperature at which the plastic enters the mould.

2.7 Overall solution algorithm

At this stage of the development an iterative scheme is used for solving the generalized Hele-Shaw flow equations because the steady-state equations are solved. The iterative solution to the flow

equations is obtained by specifying an infinite time step for the energy equation resulting in the disappearance of the time dependant coefficient A_t in Equation (2.21). A transient scheme gives the actual solution after each time step and hence a finite time step is provided. The iterative solution is equivalent to a transient solution obtained after infinite time.
The algorithm is detailed as follows:

1. Set all boundary and initial conditions.
2. Solve Equation (2.19) for pressure to give pressures at all grid points.
3. Calculate the fluxes Equation (2.24) from the pressure distribution.
4. Calculate S at each node using the quadrature formula (2.26).
5. Solve Equation (2.17) for temperature. The equation is solved iteratively until a certain degree of convergence has been reached.
6. Update boundary values.

The solution has converged once the fractional change in the pressure and temperature fields is smaller than a predetermined value. A typical value is 10^{-4}.

2.8 Solution of the discretized equations

2.8.1 Pressure equation

The matrix form of the pressure equation Eq. (2.22) is solved with a direct matrix solver (Greyvenstein and Laurie, 1994). In theory direct methods solve the problem exactly in a finite number of steps. Equation (2.18) is a Laplace equation which is being solved on a square (Figure 2.2). This gives rise to a very special but nevertheless common matrix, for which the direct solver has been optimised in terms of speed. The solver takes explicit advantage of the fact that the matrix may be partitioned into blocks, with the blocks on the diagonal all being equal.

Even though direct methods are theoretically exact, they do not achieve machine accuracy on a computer. The reason for this has nothing to do with any imperfections of such methods, but is a consequence of a very basic sensitivity theorem of linear algebra: a relative change of ϵ in the right hand side induces a relative change $k\epsilon$ in the solution where k is the condition number of the matrix (Laurie, 1983). Inevitably, therefore , no solution method, however exact in theory, can produce a solution more accurate than k times the round off level of the computer. For matrices arising from partial differential equations k usually increases as some power of the order of the matrix; e.g. for the one-dimensional heat equation $k \approx n^2$. This is not catastrophic, but neither is it negligible. For n = 100, four significant digits get lost. On a computer with a precision of 7 digits (single precision), the solution can only be accurate to 3 digits, while in double precision (14 - 16 digits) the solution can be accurate to 12 digits, (Laurie, 1983). The direct solvers are still prone to numerical round-off errors but to a lesser degree than iterative solvers. Direct solvers are more stable than iterative solvers and are faster in execution. No relaxation parameters need to be adjusted when using direct solvers which make them more fool proof. The pressure equation Eq. (2.18) is a Laplace equation and is very well suited to a direct solver. Hence a direct solver was chosen to solve the pressure, (Greyvenstein and Laurie, 1994).

2.8.2 Energy equation

In solving the energy equation (2.8), the temperature profile through the gapwise or z direction is solved using the tridiagonal matrix line algorithm (TDMA), (Anderson,Tannehill and Pletcher, 1984). The domain in the x-y plane is traversed in an alternating direction fashion from all four sides. One iteration constitutes a sweep from all four the sides of the domain. This is an iterative solver but by sweeping in all the directions it is equivalent to a direct solver and special attention needs to be paid to the initial conditions. This is only true in special circumstances such as this one. By sweeping in all the directions the number of iterations required in obtaining a converged solution are less than a

typical Gauss-Seidel solver requires. This results in less round-off errors and a quicker execution time.

2.9 Testing and calculation examples

In this paragraph the Hele-Shaw numerical scheme is demonstrated and verified by means of numerical experiments. The governing equations are programmed iteratively and tested by simulating a general case of laminar flow of a Newtonian fluid with constant density and viscosity under isothermal conditions. The results obtained from these simulations are compared to analytical solutions of the simplified Navier Stokes equations. The Hele-Shaw numerical scheme is then tested on a symmetrical geometry and the results tested for symmetry.

2.9.1 Pressure gradient tests

The relationship between the pressure drop along the length of the domain, shown in Figure 2.2, and the flow rate is compared to an analytical relation (Shames, 1982). The influence of the number of grid points on the accuracy of the pressure solution is also investigated. The pressure is two-dimensional and only varies in the x-y plane. The grid shown in Figure 2.2 is divided into 12 nodes in the x direction, 6 nodes in the y direction and 10 nodes in the gapwise z direction for the first set of numerical experiments. For the second set of experiments a finer grid was chosen with 18 nodes in the x direction and 8 nodes in the y direction. Isothermal non-Newtonian flow is considered here, hence the number of grid points in the gapwise z direction has no influence on the accuracy of the solution because S is a constant and no integration is being done in the z direction.

For the analytic relation the flow in the x-z plane Figure 2.5 is considered with a constant depth Y in the y direction. This reduces to flow between two parallel plates that are separated by a distance of twice the half gap width b. The analytical relation is given by (Shames,1982)

$$\Delta p = \frac{3 q L \mu}{2 b^3 Y} \qquad (2.27)$$

where L is the length across which Δp is measured and Y is the depth in the y-direction.

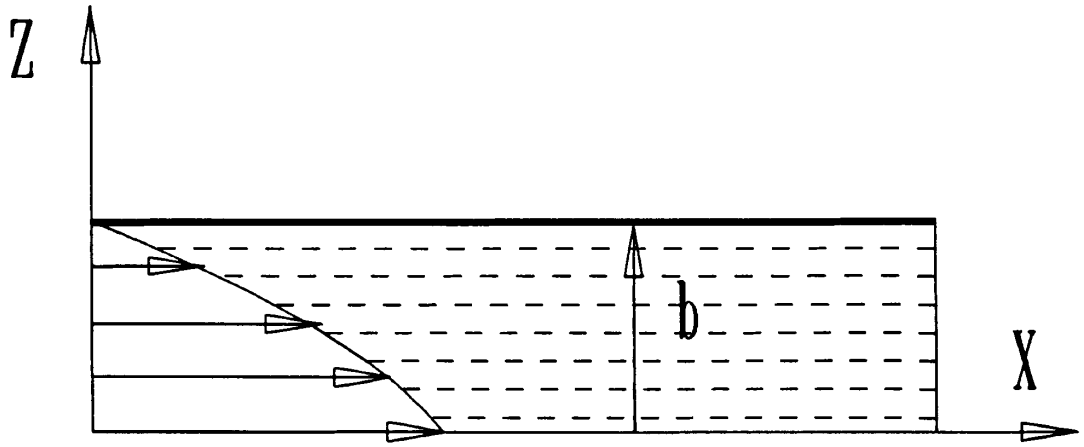

Figure 2.5. Flow between parallel plates.

Various flow rates were considered and the corresponding pressure gradients were calculated from relation (2.27). The results are presented in Figures 2.6 and 2.7 in non-dimensional form which gives a more general representation of all the variables over the specified range. The pressure drop is represented by the Euler number (Eu) which represents the ratio of the pressure force to the inertia force. The Euler number is given by

$$Eu = \frac{\Delta p}{\rho V^2} \qquad (2.28)$$

where V is the velocity.

The varying flow rate is represented by the Reynolds number (Re) which represents the ratio of the inertia force to the friction force. The case that was chosen Figure 2.2 has a constant velocity in the x direction which is calculated from the volumetric flow rate and used in the Reynolds number. The hydraulic diameter of the mould was used for the length dimension. The Reynolds number is given by

$$Re = \frac{\rho V L}{\eta} \tag{2.29}$$

It can be seen from Figures 2.5 and 2.6 that an excellent correlation is achieved between the results of the Hele-Shaw flow model and those from the analytical relation given by Equation (2.27). The percentage error between the two methods is constant for both grid densities and is 5,7% for the 12 by 6 grid and 3,8% for the 18 by 8 grid. Theoretically a grid independent solution can be obtained, ie a 0% error, by making the grid even finer but this is impractical due to the memory limitations imposed by computers on numerical methods. These tests have shown that the Hele- shaw flow results are acceptable in terms of accuracy and this was the aim of the tests.

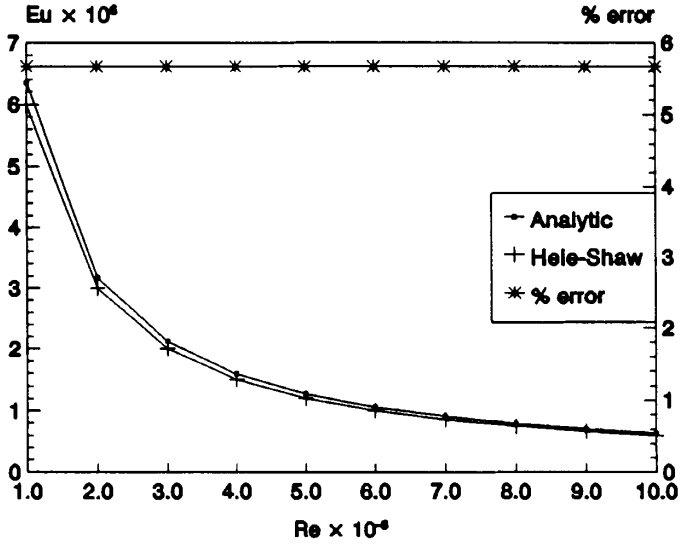

Figure 2.6. Euler number vs Reynolds number for a 12 by 6 grid.

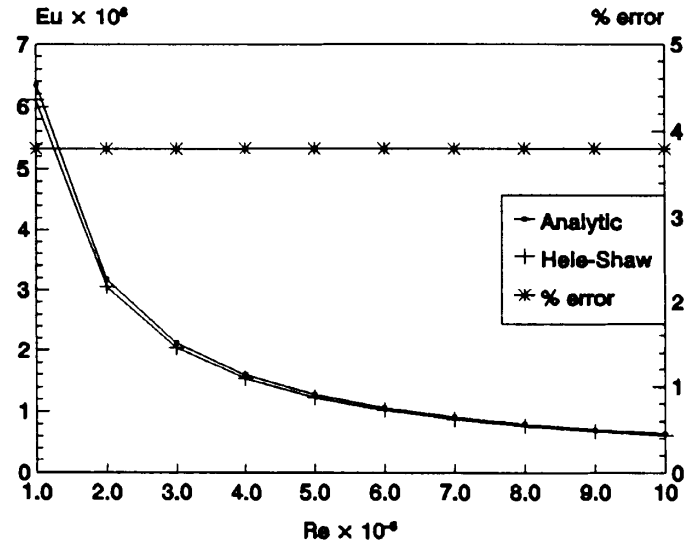

Figure 2.7. Euler number vs Reynolds number for a 18 by 8 grid.

2.9.2 Pressure field symmetry tests

Hot molten plastic is extremely viscous and is also a non-Newtonian fluid. This results in huge pressure, viscosity and temperature gradients which are difficult to simulate without having numerical round-off errors that have a detrimental effect on the overall accuracy of the solution. The precision of the floating point numbers can be set on the particular compiler that is used and this choice effects the accuracy of the solution in terms of numerical round-off errors. More memory is required for higher precision representation of the floating point numbers and so a compromise has to be reached in terms of precision and accuracy.

The best method to investigate numerical round off errors is to simulate a typical case on a symmetric domain and check whether the results obtained are symmetrical. An isothermal Newtonian fluid with a viscosity that corresponds to an average viscosity in the gapwise z direction of a typical plastic is used in this experiment. This will ensure that the orders of magnitude of the pressures will be the same as those used if a proper material model was already incorporated. The material model is temperature dependant and indirectly dependant on the movement of the free front, hence tests on the energy equation will not be incorporated at this stage of the development.

The symmetry tests are performed on a square 50mm mould shown in Figure 2.8 which is divided into 19 grid points in both the x and the y directions. The boundary conditions, the point of injection and the line of symmetry are shown in Figure 2.8. The floating point numbers are all declared with double precision in the program. The pressures along the x axis and the y axis are recorded and due to the problem being symmetric they are expected to be identical. The percentage error between the two is calculated and plotted in Figure 2.9 along with the actual pressures. It can be seen from Figure 2.9 that at this stage of the development the pressure distributions are perfectly symmetric along the x and y axes of Figure 2.8. The percentage error is insignificant at all points. This test proves that the

numerical scheme is accurate to within computer limits at this stage of its development. This test will be repeated with the incorporation of the free front and the inclusion of the material model so that the loss in accuracy can be observed.

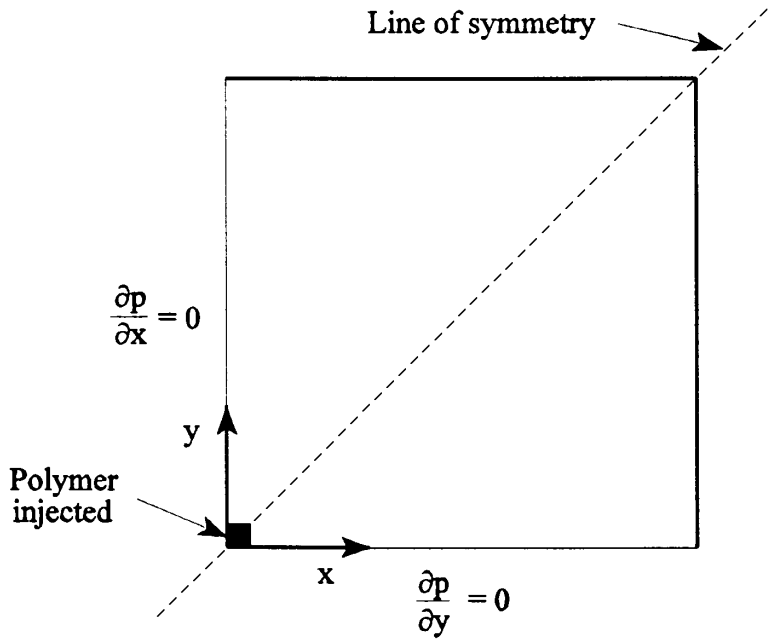

Figure 2.8. Mould indicating computational domain for symmetry tests.

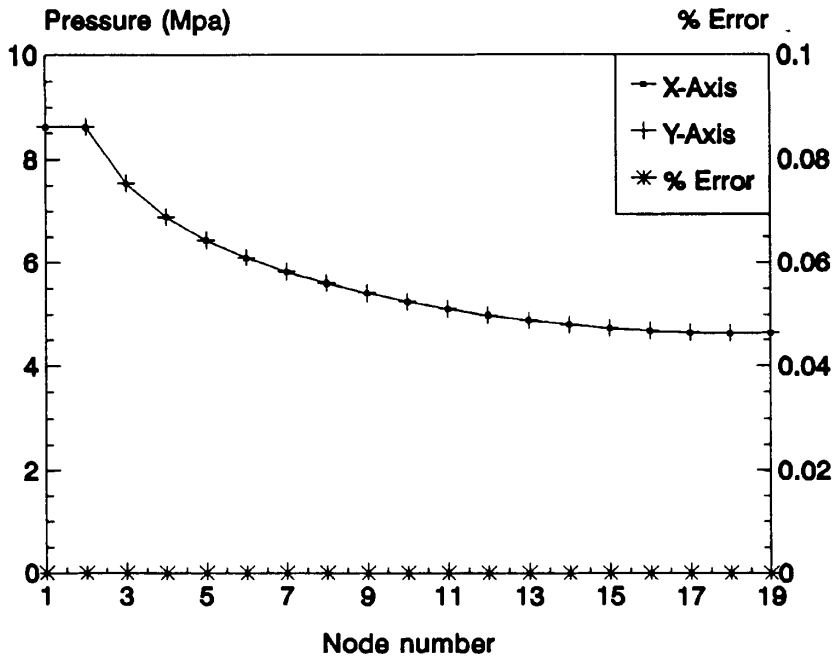

Figure 2.9. Pressure distribution along the x and y axes for symmetry test

2.9.3 Energy equation solutions

Only a Newtonian isothermal fluid with a constant density is being considered at this stage of the development. The energy equation is introduced in this chapter and for completeness tests are performed which investigate the effect of using the local velocity Eq.(2.7) or the mean velocity Eq. (2.8) formulation of the energy equation. Figure 2.10 shows that at this stage of the program's development there is no difference between the local velocity formulation or the mean velocity formulation. The numerical scheme and temperature solving routine of the energy equation can only be examined. From Figure 2.10 it can be seen that the numerical formulations are correct. Once the material model is introduced in Chapter 3, the program will be able to deal with non-Newtonian

thermal flow and the effects of using the mean velocity formulation instead of the local velocity formulation in the energy equation will once again be investigated.

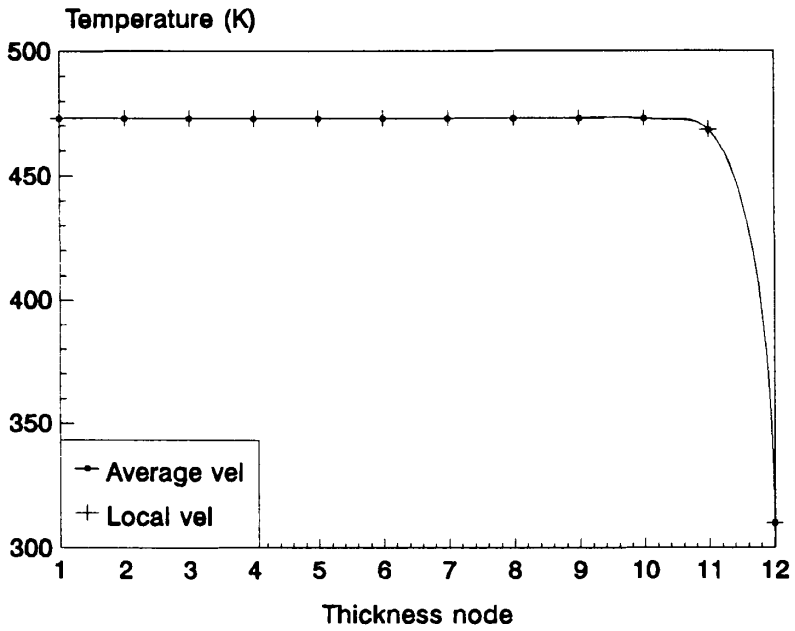

Figure 2.10. Energy equation formulations using the local velocity or the mean velocity in the convective term.

The volumetric flow rate fluxes, i.e. Fe, Fw, Fn and Fs given by Eq. (2.24) were also summed for each control volume. For continuity to be satisfied the sum of these fluxes has to be zero on each and every control volume except for the control volume where the hot melt is injected into. The sum on this control volume has to be the same as the constant volumetric flow rate with which the melt is entering the mould. With all the tests that were performed with the program, continuity was maintained in the above mentioned way hence the numerical scheme satisfies continuity.

The literature survey revealed that no results are recorded for a Hele-Shaw numerical scheme at this stage of its development. The numerical experiments that were performed in this paragraph are sufficient to warrant the extension of the program to include an algorithm for the tracking of the free front.

2.10 Closure

In this chapter the Hele-Shaw flow equations were introduced. A finite volume method was chosen above the finite element method for the development of the code. The governing equations were discretized and programmed using a direct solver for the pressure equation. The energy equation was programmed using the Thomas line by line solver in conjunction with an alternating direction Gauss-Seidel iterative scheme. At this stage of the program's development the material model has not been incorporated yet which is very temperature dependant. Hence the energy equation algorithm still has to be tested in the next chapter once the material model has been incorporated. An integration quadrature formula was introduced and discussed for calculating S in the gapwise direction. Results were obtained and discussed for the Hele-Shaw numerical scheme that is solved iteratively for an isothermal incompressible Newtonian fluid. The results compare favourably with analytical relations that are derived from the Navier-Stokes equations. There is no literature available with results at this stage of the program's development for comparison but tests showed that all the fundamental equations are accurately solved. Problems encountered in the development of the code were highlighted. The results and correlations obtained in this chapter warrant further development and in the following chapter an algorithm for the tracking of the free front will be discussed. An appropriate material model for the calculation of the viscosity will also be discussed and included into the program.

3 FREE SURFACE MODELLING

3.1 Introduction

In Chapter 2 the numerical scheme for the Generalized Hele-Shaw model was developed and applied to steady continuous flow through a thin gap to test and verify the basic scheme. The movement of the free flow front was not considered. The basic numerical scheme was developed and tested. A material model was not incorporated and extremely viscous Newtonian flow was considered. This was to test the basic numerical scheme.

In this chapter the literature survey is reassessed with regard to the modelling of the movement of the free front. Various methods have been proposed and these are discussed critically. Once again a method is chosen for this program that best suites the objectives. The method is discussed in detail and the appropriate governing equation is discretized on a rectangular Cartesian domain and implemented. Time dependant flow through a rectangular cavity, representing a mould for a typical thin walled product is considered. Isothermal Newtonian flow is first considered and after this has been tested and verified a suitable material model is incorporated. Associated problems are identified and solved.

Finally the method is tested and verified for non-isothermal non-Newtonian flow before proceeding to chapter 4 where the model is extended to incorporate general curvilinear coordinates.

3.2 Background

In a moving boundary problem, part of the boundaries move according to prescribed kinematic and dynamic conditions. Since the location of the free surface is an additional degree of freedom, at least one more equation with one more dependant variable is needed than in a problem with fixed boundaries. There are many different algorithms for tracking moving boundaries depending upon the

choice of the numerical method, finite element or finite volume. Most numerical tracking methods are of two categories, Eulerian or Lagrangian, both of which will be explained briefly.

The Lagrangian method may be more precise in a mathematical sense, but it consumes a lot of CPU time and is not necessarily robust in a practical sense because it requires to move the nodal points and to remesh or regenerate the flow field in accordance with the melt front advancement. The Eulerian method is inferior in mathematical exactness, but it has the advantage of a fixed mesh and is considered to be preferable for the development of commercial codes because it is adaptable to any complex geometrical shape. For these reasons a Eulerian mesh is most suited to our applications.

In the literature survey various numerical tracking methods were mentioned and reported on. One of the earliest methods used in tracking the front was the branching flow approach but this has been rejected by most researchers. The Marker-and-Cell (MAC) method is very popular and was developed to study transient incompressible viscous flows with free surfaces in the field of hydraulics. An extended version of the MAC method simulates the fountain flow effect of non- Newtonian fluid flow applied to two-dimensional (x-z plane), isothermal filling processes of simple geometries- parallel plate and radial flows (Hirt and Nichols, 1981). The MAC method utilises a fixed Eulerian mesh for finite difference calculations and a Lagrangian set of marker particles to delineate the moving free surfaces. A staggered grid system is used in which the velocity components are centred at the cell boundaries and pressures placed at the cell centres for better accuracy. First, the coordinates of marker particles representing the fluid domain are stored. After the velocity field is calculated marker particles are then moved with a weighted average of the four nearest cell velocities. At this time the cells are properly flagged as empty, full or surface cells depending on the distribution of marker particles. This cell information will be used to define the boundaries of the flow domain for the next time cycle. This technique has been especially useful for analysing the fountain flow

phenomena in the x-z plane. It is, however, difficult to use the MAC method to simulate the filling process of complex moulds without making major extensions. The method also suffers from a significant increase in required computer storage and it also requires additional computer time to move all the markers to new locations.

According to the literature survey, it is noted that most of the modern day commercial packages utilise the Hele-Shaw approach in conjunction with the Flow Analysis Network (FAN) approach for tracking the free front. This approach has extended the MAC concept into the low Reynolds number flow regime (such as the plastics filling process), using lubrication theory in the (x-y plane) instead of the Navier Stokes equations, which is the Hele-Shaw approach. In terms of free surface tracking, FAN uses the flux calculations at the boundary of each control volume to check the fraction of fill in order to trace free surfaces instead of tracking marker particles. One limitation of this control volume approach is that the time steps must be controlled to ensure that the free surfaces pass only one layer of control volumes in one time step. A scheme to correlate the time steps and the flow front control volumes was implemented in the (FAN) program (Hieber and Shen, 1980). The use of a global coordinate system and multi dimensional indexing within the context of the finite difference method causes two major problems in using the technique to simulate mould filling. In addition to the tedious layflat, which is a procedure to unfold any 3-D part onto a 2-D plane, a great amount of additional data on the joint nodes which connect the planes of the model must be entered. This method is well suited to the finite element method but not to the finite difference method.

The Volume-of-Fluid method (VOF) was developed by Hirt and Nichols (1981) for the purpose of sharing the region defining property of the MAC approach but without its excessive computer storage requirements. This method is based on the same concept as the FAN approach. In each control volume a single value is used for defining its state of concentration. We define a function C whose

value is unity at any volume occupied by fluid and zero if empty. The average value of C in a volume then represents the fractional volume of the cell occupied by fluid and if it is between 0 and 1 then the volume must contain a free surface. Thus this method provides the same coarse interface information available to the marker particle method, but requires only one storage value for each volume which is consistent with the storage requirements for the other dependant variables.

By looking at all the methods that were presented in the literature survey and reassessed in this chapter the VOF method is best suited to serve the objectives that were stated in Chapter 1. The fact that this method uses relatively little memory, makes it the best suited method for a personal computer. The VOF method can be applied to finite volume techniques with ease whereas the other methods are better suited to finite element formulations.

3.3 Governing equation

The Volume-of-Fluid technique can locate free boundaries nearly as well as a distribution of marker particles and with a minimum of stored information. The distinctive nature of a free front model lies in the nature of the algorithm itself and not so much on how it is solved, be that with a finite element or finite volume method. A solution algorithm must be devised for accurately computing the evolution of the concentration field C. The time dependence of the concentration C is governed by setting its substantial derivative equal to zero:

$$\frac{\partial C}{\partial t} + \bar{u}\frac{\partial C}{\partial x} + \bar{v}\frac{\partial C}{\partial y} = 0 \qquad (3.1)$$

where C = 1 is in the fluid, C = 0 is in a void and where C = 0.5 represents the free surface. This equation can also be derived by considering mass conservation. This equation states that C moves with the fluid and is the partial differential equation analogue of marker particles. In our application

C serves solely as a function identifying cells that contain fluid. Continuity is always satisfied meaning that equation (3.1) can also be written in conservative form. The advantages of writing the governing Equations in conservative form were discussed in Paragraph 5.2 of Chapter 2. The resulting equation in conservative form is given by

$$\frac{\partial C}{\partial t} + \frac{\partial(\bar{u}C)}{\partial x} + \frac{\partial(\bar{v}C)}{\partial y} = 0 \qquad (3.2)$$

An algorithm for the tracking of the free front has now been identified and discussed. The governing equation must now be discretized and a suitable solver must be identified.

3.4 Discretization of the Concentration equation

The concentration equation Eq. (3.1) implies that the concentration is transported by convection because no diffusion terms are present. If the cell Reynolds number or the Peclet number exceeds 2 which will always be the case because the diffusion coefficient is zero then central differencing causes the algorithm to be unstable, hence upwind differencing will be required. The disadvantage of upwind differencing is that it gives rise to numerical diffusion whereas central differencing defines the position of the free front more clearly. The disadvantage of central differencing is that dispersion occurs at the free front making the algorithm unstable. This means that to use upwind differencing is not so critical with plastic flows and in this chapter central differencing and hybrid central/upwind differencing schemes will be investigated.

3.4.1 Implicit discretization

The concentration equation in conservative form Eq. (3.2) is discretized using upwind differencing according to the grid shown in Figure (2.3) and the resulting differential coefficients Equation (2.17) are given by:

$$\left.\begin{aligned} A_E &= \max(0,-F_e) \\ A_W &= \max(0, F_w) \\ A_N &= \max(0,-F_n) \\ A_S &= \max(0, F_s) \\ A_t &= \frac{\Delta x \Delta y}{\Delta t} \end{aligned}\right\} \tag{3.3}$$

where the volumetric flow rate fluxes are defined by Equation (2.24). Due to the implicit method being used the concentrations that appear in the final dicretised concentration Equation (3.4) are all taken at the new time step, except for the time dependant term. The final implicit discretized concentration equation is given by

$$(A_P + A_t)C_P^t = \sum A_{nb}C_{nb}^t + A_tC_P^{t-1} \tag{3.4}$$

The advantage of an implicit formulation is that it is unconditionally stable. The disadvantage of the implicit method is that it requires more iterations to converge and numerical round-off errors could render the solution inaccurate. The upwinding in the implicit formulation could also tend to smear the front slightly.

3.4.2 Explicit formulation

For the explicit formulation the resulting differential coefficients are identical to those of the implicit method Equation (3.3). The only difference being that the final discretized concentration equation is written in terms of the concentrations at the previous time step. The final explicitly descretised equation is given by

$$A_tC_P^t = \sum A_{nb}C_{nb}^{t-1} + (A_t - A_P)C_P^{t-1} \tag{3.5}.$$

The explicit method is only conditionally stable and the time step must be smaller than a certain value to ensure stability.

3.4.3 Hybrid formulations

The hybrid formulation is a combination between upwind differencing and central differencing. A parameter α is used to define the fractional amount of upwind differencing in the formulation and (1-α) the fractional amount of central differencing in the formulation.

With upwind differencing the volumetric flux across the face of the control volume in question is considered. The sign of the flux, i.e. + or -, indicates the direction of the flow across the control volume face. The upstream control volume's concentration is always used as the concentration on the control volume's face in the formulation. Whichever control volume's concentration was chosen as the concentration for the particular control volume in question's face is then multiplied by the parameter α.

With central differencing the concentration at the control volume's face is always taken as the mean between the particular control volume's concentration and that of the neighbouring control volume. This concentration is then multiplied by (1-α) and then added to that obtained from the upstream differencing to get the concentration that will be used in the formulation.

For the hybrid implicit formulation Equation (3.4), and for the hybrid explicit formulation Equation (3.5), will be used to describe the concentration equation in descritised form. The above mentioned procedure is used for calculating the coefficients A_{nb} in these two equations. The coefficients A_{nb} in Equations (3.4) and (3.5) are the volumetric fluxes across the faces of the control volume leading into the control volume.

The central differencing portion of the hybrid scheme produces a much sharper front but causes fluctuations or oscillations at the interface. The upwind differencing tends to smear the front over more cells or control volumes. The upwinding also contributes to the hybrid solution being more stable.

3.5 Boundary conditions

The boundary conditions for Equation (3.2) are as follows. A value of C = 1.0 is specified at the inlet and C = 0.0 at all other positions on the domain. At all other boundaries the concentration equation adopts the same type of boundary conditions as those of the pressure equation at the same boundary. The concentration also dictates the pressure equation's boundary conditions at solid walls. The pressure equation which is a Laplace equation has a Dirichlet boundary condition, i.e. $P= P_{atm}$, at solid walls that are not yet in contact with material. Once the material is in contact with the wall the boundary condition becomes a Neumann type and the boundary condition is a zero pressure gradient corresponding to a zero velocity. The Laplace equation requires at least one Dirichlet boundary condition to solve and when the last Dirichlet boundary condition disappears the mould is full and the filling stage is complete. This stopping criteria is verified analytically by dividing the volume of the mould by the constant flow rate and obtaining a filling time.

3.6 Transient time increment

In transient problems, the time increment affects the accuracy and stability of the solution. The time step becomes a very critical factor for the Hele-Shaw flow problem using the Volume-of-Fluid (VOF) method for tracking the free front. For solution stability the free front is not allowed to advance more than one grid spacing in a single time step. The VOF method dictates that a time increment must be chosen such that the Courant number Co is smaller than 1. The Courant number is given by

$$Co = \frac{U\Delta t}{\Delta x} \tag{3.6}$$

where U is the magnitude of the velocity and Δt and Δx are the time step and the mesh size, respectively. A Courant number less than unity, corresponds to a flow front displacement less than Δx over the time increment Δt. By choosing $Co < 1$ gives stable flow front advancement.

In the program the time increment is not chosen arbitrarily and kept constant for the entire transient simulation. A new time increment is re-calculated after each time step by examining the amount of volumetric flux entering each and every control volume. The amount of flux entering a control volume across all four faces is added up and divided into the volume of the particular control volume. By dividing the internal volume of the mould by volumetric flow rate of the melt entering the mould a time increment is obtained. This time increment is once again multiplied by a time factor, typically 0,7, which ensures that the free front does not move the entire length of that particular control volume in the next time step. This procedure is performed on all the control volumes in the domain and the smallest time increment is used as the next time step for the program. This method also ensures that the Courant number is always smaller than unity.

3.7 Modifying the pressure solving routine

The following has already been mentioned in the literature survey in Chapter 1 but for completeness it will be repeated again. It was mentioned that when using a finite element method creeping viscous flows are followed through meshes by means of pseud concentrations which are used to define the position of the free front. The concentrations, which are assumed to be transported by convection alone, serve as material markers. The classical VOF method Equation (3.1) discretized using finite differences has been applied to injection moulding problems where the pressure equation, Eq. (2.18),

is solved with the finite element method giving rise to a hybrid formulation. The VOF method is best suited to an Eulerian scheme where a pseud concentration is assigned throughout the entire mesh in such a manner that its value indicates the presence or absence of creeping viscous material. In regions where the material is present, the appropriate effective viscosity is used during the assembly of the stiffness matrix. In those regions of the mesh where the value of the concentration indicates that the material has not yet penetrated, an artificially low value of the viscosity is used so as not to affect the velocity of the higher viscosity material. However, if too low a value is specified for the viscosity of the artificial material the finite element equations become ill conditioned. The artificial viscosity of the fluid must be two orders of magnitude less than the real fluid for numerical stability in finite element meshes (Thompson, 1986).

To incorporate the moving front into the pressure equation Eq. (2.18), the viscosity was multiplied by a smaller number than was recommended by Thompson ($\approx 10^{-6}$), in those regions where the material is not present yet. The reason for using a smaller number than was recommended by Thompson is that a different solution algorithm is used for the concentration equation in the finite volume method which does not give problems when the viscosity in the void space becomes too small. The solving methodology of a finite volume method is less complicated than that of a finite element method because finite element formulations have interpolation functions with stiffness matrices that can become ill conditioned. For this reason the pseud viscosity can differ from the material viscosity by orders of magnitude greater than two and the overall solution will still be stable.

This modification to the viscosity results in the pressures being atmospheric in the regions where the front has yet to pass, and actual pressures are assigned to those regions where the material is present. This method of incorporating the moving front into the pressure equation is compatible with the overall numerical scheme.

3.8 Smoothing the Coefficients

The coefficients given by Equation (2.20) of the pressure equation Eq. (2.18) need to be modified at the control volumes where the front is passing through at a particular time step. The front does not jump from one node to another during a time step but moves in a continuous fashion. Hence at certain time steps the front will lie between two nodes and the pressure coefficients have to be adapted accordingly. A specific control volume can only contain plastic melt or the pseud fluid with a viscosity much lower than the melt. A linear interpolation function is used on the values of C to obtain the precise position of the front, i.e. where C = 0.5 between two nodes. Once this position has been determined the respective control volume's Δx's and Δy's are modified resulting in altered pressure coefficients at the front. This enhances the accuracy of the overall Eulerian method but is still not as accurate as a Langrange formulation will be, where the entire mesh or grid is regenerated after each time step. The same procedure is applied when calculating the volumetric flow rate fluxes, Equation (2.24).

In Figure 3.1 isothermal Newtonian flow on the domain shown in Figure 2.8 is considered to demonstrate the effect of smoothing the coefficients. The pressure build-up at the inlet is monitored after each time step for 30 time increments. The case where the coefficients were not smoothed shows that the pressure builds up in a discontinuous manner with time. The reason being that the pressure equation sees the front as jumping from node to node in the domain where it actually moves in a smooth continuous way. After the pressure coefficients and the volumetric flow rate flux equations were modified to incorporate the movement of the free front the pressure build-up became a continuous function. From Figure 3.1 it can be concluded that the smoothing of the coefficients is vital for ensuring an accurate and realistic simulation.

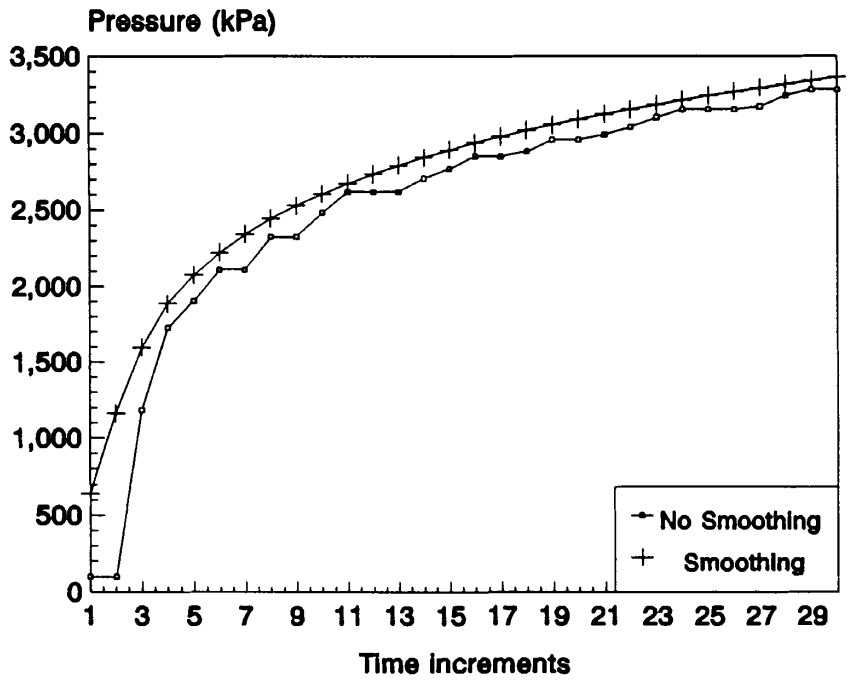

Figure 3.1. Pressure build-up at the inlet demonstrating the effect of smoothing the coefficients.

3.9 Diffusive nature of the front tracking equation

3.9.1 Background to the problem

In an Eulerian mesh the convective flux which flows through the mesh requires an averaging of the flow properties of all the fluid particles that find themselves in a given control volume after some period of time. It is this averaging process inherent in convective flux approximations, that is the biggest drawback in Eulerian methods. Convective averaging results in a smoothing of all variations in flow quantities, and in particular a smearing of surfaces of discontinuity such as free surfaces.

Since C in Eq. (3.1) is the only available free surface information, an approximate reconstruction of the free surface must be performed to obtain the free surface location. Sharp interfaces are maintained by insuring sharp gradients in C. This is achieved by a simple procedure that will be explained in the next section. A standard discretization of Equation (3.1), especially an upwind approximation, leads to an unacceptable amount of numerical diffusion which spreads the free surface region. An approximate reconstruction is necessary for maintaining an accurate representation of the front.

The only way to overcome this loss in resolution for free boundaries is to introduce some special treatment that recognizes a discontinuity and avoids averaging across it. With the finite volume representation of the Hele-Shaw flow equations zero gradient boundary conditions are applied to all the dependant variables across the free front. The position of the free front is identified where C = 0,5 and all the values of the flow variables behind the front are assigned to the points just ahead of the front so that the discontinuity does not influence further calculations. Thus if the free front is spread out over a wide region accuracy is lost.

3.9.2 An algorithm for the sharpening of the free front

Hirt and Nichols (1981) presented a differencing scheme for C which eliminated the diffusion caused by upwinding the convective concentration equation. In the program another method of combating the unwanted diffusion is proposed and if unsuccessful the Hirt and Nichols method will be used. The Hirt and Nichols method is more complex and memory intensive than the method that is going to be proposed.

In order to minimise the numerical diffusion an algorithm was developed that accurately identified the position of the front and corrected the concentrations accordingly after each time step. This

algorithm operates independently from the concentration solving algorithm and can be deactivated if not required.

The flow variables including the concentration are solved for a particular time step and the concentration distribution is available. The algorithm then identifies the position of the free front by marking its adjacent control volumes and these volumes are referred to as the boundary volumes. The concentration values C of these two volumes are kept constant so as not to disturb the concentration gradient across and the position of the free front. The values of concentration ahead of the front excluding the boundary volumes i.e. where $C < 0,5$, are taken and distributed evenly behind the front, once again excluding boundary volumes, where the concentration values are $C < 1$ and $C > 0,5$. However, situations do arise where concentration needs to be added to the boundary volumes. When this occurs concentration is distributed evenly to the two adjacent boundary volumes so as to maintain the original concentration gradient across the free surface and therefore the exact position of the free surface. Only the concentration ahead of the free front is packed back. The concentration variable C is conserved at all times in this algorithm. This means that there is never a loss or build-up of concentration and hence the calculation of the filling time will not be influenced. With the hybrid discretization methods i.e. where central differencing is used, dispersion also occurs at the free front interface. Dispersion causes the values of concentration C to oscillate near the free front interface and the values of concentration may exceed 1,0. The packing algorithm also corrects these "wiggles" which may occur by taking the concentration that has diffused ahead of the front and placing it back behind the front.

Figure 3.2 demonstrates the packing algorithm and once again isothermal Newtonian fluid is simulated on the geometry presented in Figure 2.8. The program was executed using the hybrid implicit method for solving the concentration equation. The line of symmetry shown in Figure 2.8 was

used for observing the motion of the free front. Once the free front had moved to half way between the point of injection and the furthest corner the program was stopped and the values of concentration along the line of symmetry recorded. The concentration distribution was then modified by the packing algorithm and the results recorded and presented in Figure 3.2.

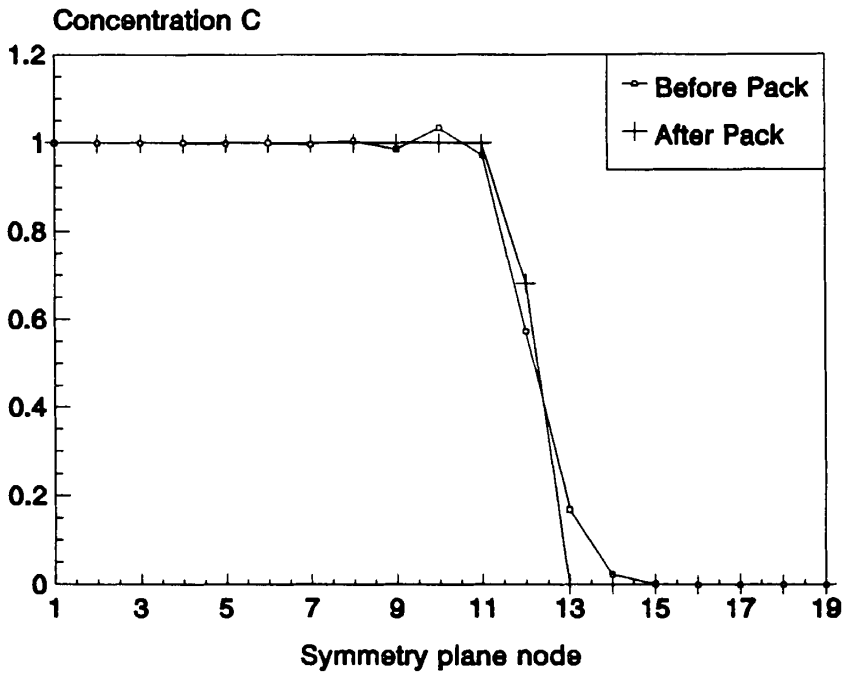

Figure 3.2. Concentration distribution along the symmetry line before and after packing.

As can be seen from the figure the packing algorithm eliminates the dispersion and gives the free front a much sharper definition by reducing the unwanted effects caused by diffusion. It can also be seen that the packing algorithm does not change the exact position of the free front i.e. the position where the concentration C is equal to 0,5. It can be concluded that this packing algorithm is successful in reducing the amount of unwanted diffusion and can be used with confidence in the program.

3.10 Example Calculations

In this section the Hele-Shaw numerical scheme with the free front is demonstrated and verified by means of numerical experiments. The flow equations are solved transiently, as opposed to iteratively in Chapter 2, and the Volume-of-Fluid method is used for tracking the free front. The scheme is once again tested by simulating a general case of isothermal Newtonian flow with constant density on the geometry shown in Figure 2.8. The different formulations of discretising Equation (3.1) are detailed in Paragraph 3.4 and the results of these formulations are compared to each other and discussed. The simulations are performed with and without the packing algorithm in order to find the best method for the tracking of the free front. This method is then selected for taking the program into its next stage of development.

The movement of the free front is tested by allowing the free front to move to half way between the point of injection and the furthest corner of the mould. Once this point has been reached the program is halted and the position and cross section of the free front examined. All the formulations are stopped after the same time so as to get an accurate comparison. The concentration values are then plotted along the line of symmetry at each node, obtaining the concentration cross section. The position of the free front on the x-y plane is also recorded and plotted. This is done by plotting the curve C = 0,5 on the x-y domain presented in Figure 2.8. After these results were recorded the identical simulations were repeated with the packing algorithm activated, packing the concentration behind the free front after each time step.

By examining Figures 3.3 and 3.4 it can be seen that the hybrid explicit, hybrid implicit, explicit and implicit formulations all predict the free front to be at exactly the same position. It can be seen from Figure 3.3 that the hybrid formulations are characterised by dispersion or "wiggles" near the free front interface. Figure 3.5 demonstrates how the packing algorithm sharpens the free front and eliminates

the dispersion caused by the central difference blend in the hybrid methods without altering the position of the free front i.e. where C = 0,5. The comparison between Figures 3.3 and 3.5 demonstrates how the packing algorithm provides the position of the free front with a much sharper definition without altering its position. Figure 3.6 shows how the free front traverses the domain and shows how the circular path is maintained during the filling stage indicating that the algorithm is correct. It is concluded that the packing algorithm is not essential but definitely eliminates the numerical diffusion after each time step, producing a better and more accurate solution.

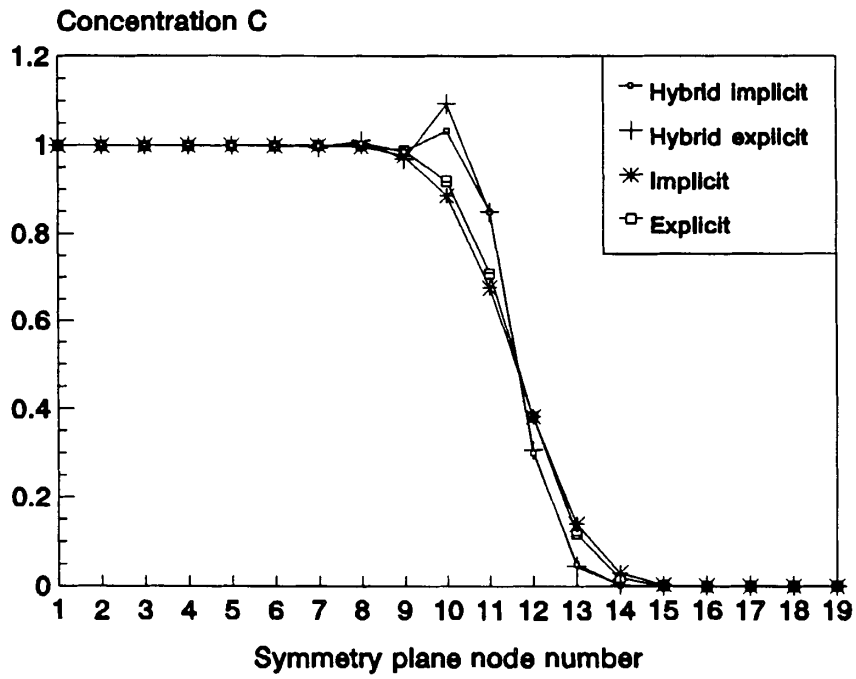

Figure 3.3. Concentration distributions of the various methods along the line of symmetry without packing.

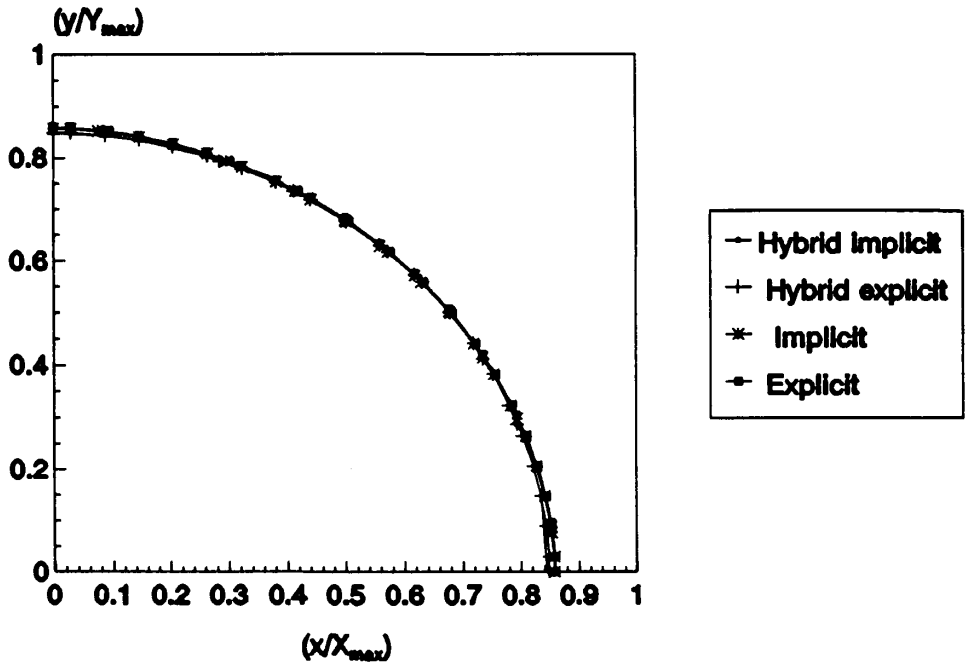

Figure 3.4. Positions of the free front using the various methods on the x-y plane without packing.

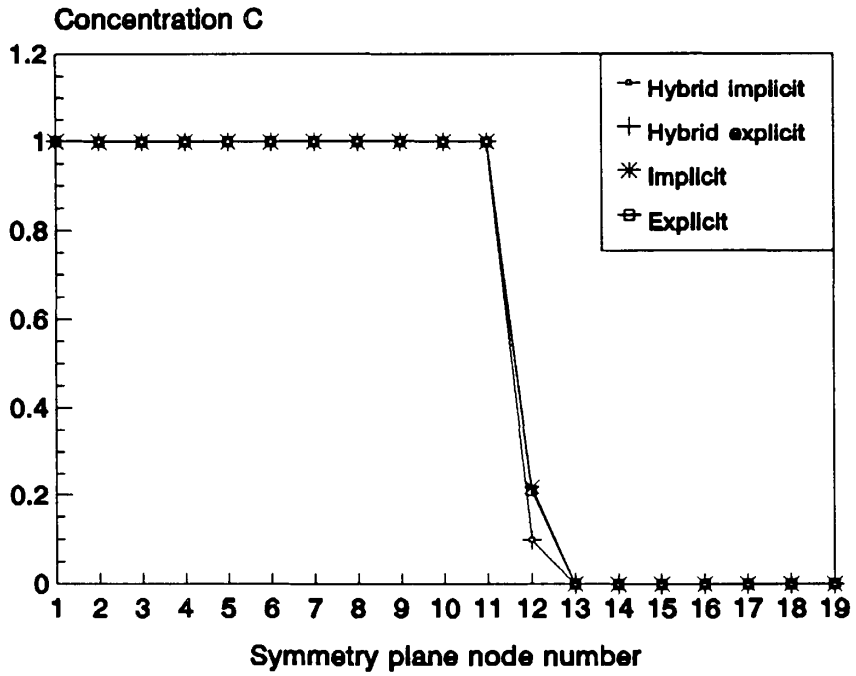

Figure 3.5. Concentration distributions of the various methods along the line of symmetry with packing.

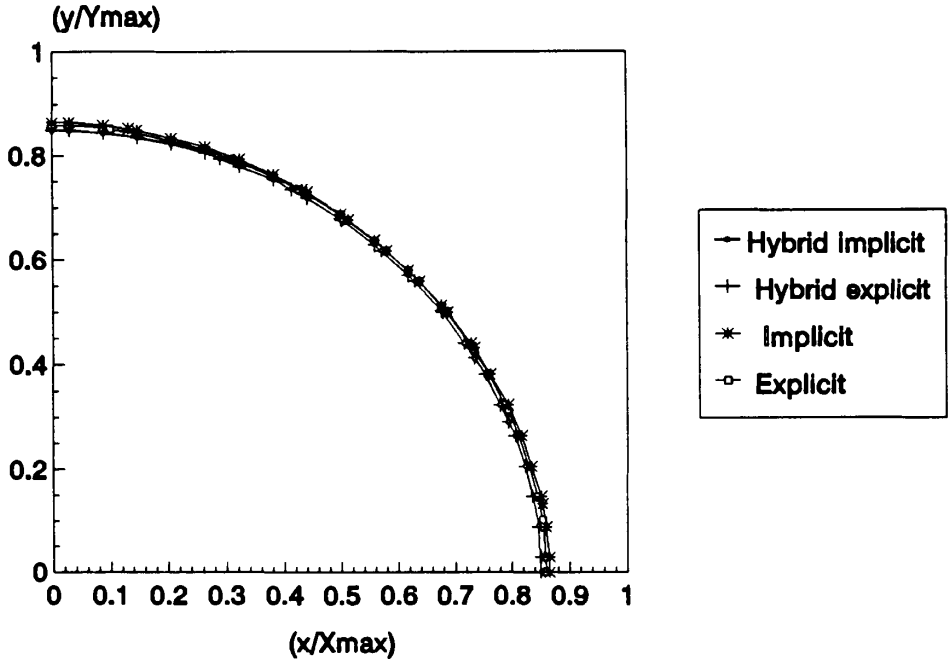

Figure 3.6. Positions of the free front using the various methods on the x-y plane with packing.

Figure 3.7 is a plot of the free front advancement along the line of symmetry (Figure 2.8) taken after each time step till fill time is reached. The y axis represents the distance r in non dimensional form, from the point of injection along the line of symmetry to the furthest corner denoted by R_{max}. The x axis denotes the number of time steps taken to reach the respective position. It is seen from Figure 3.7 that all the formulations predict the free front to have moved the same throughout the filling time range. The various predictions are very close together and significant variations only occur at and around fill time. All the formulations are within 2% of each other which is entirely acceptable.

All the discretization formulations presented in this chapter provide excellent results and it is impossible to single a method out as producing the best results. Theoretically the implicit formulations are unconditionally stable whereas the explicit formulations are only conditionally stable. Due to the highly non-linear behaviour of the non-Newtonian fluid, plastic, it is wise to choose an implicit formulation. The hybrid formulations are less diffusive and provide a much sharper interface which is confirmed by the results obtained in Figure 3.3. Therefore theory dictates that the safest method is the hybrid implicit formulation. The other formulations will not be discarded at this stage of the development and are left as an option for the user when doing a simulation even though the recommended formulation is the hybrid implicit with packing.

The constant volumetric flow rate with which fluid is injected into the mould is divided into the internal volume of the mould to obtain the filling time. The free front using the hybrid implicit formulation traverses the entire mould in exactly that time hence the method is accurate.

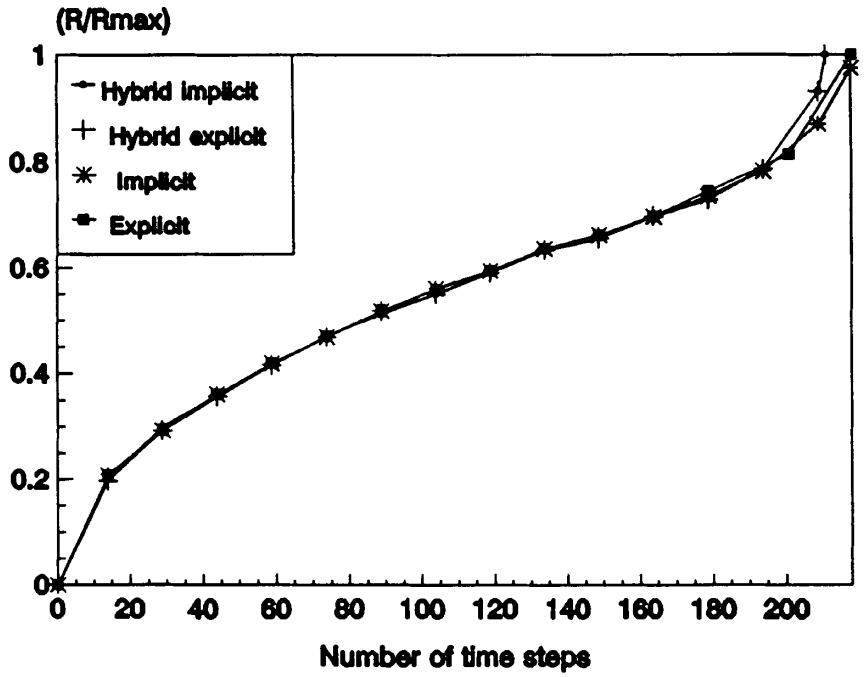

Figure 3.7. Position of the free front along the line of symmetry versus time with packing.

3.11 Material model

3.11.1 Introduction

The accuracy of an injection moulding simulation depends to a large degree on the model used for viscosity. A realistic simulation requires that the viscosity be well characterised in terms of its dependence upon shear rate, temperature and pressure in order to calculate S given by Equation (2.16). The literature survey in Chapter 1 reviewed previous research in this field.

One evident characteristic exhibited by the shear viscosity of polymer melts is a shear thinning behaviour with increasing shear rate. The viscosity of such materials is highly dependant upon temperature and pressure. An understanding of the viscous behaviour of a polymeric material is necessary in order to relate the stress to the deformation rate. For the case of a simple low molecular weight Newtonian fluid, a single experiment suffices to determine the viscous behaviour of the system. However, for viscoelastic polymer melts the viscous behaviour of the material is vastly more complicated. Simple experimental tests have been devised which yield well defined material functions or viscous properties which are used for computational purposes. The material model is very empirical in nature and past research into various materials is relied upon.

The literature survey indicates that Wang and Hieber (1988) have done the most research into this field as part of the Cornell Injection Moulding Program (CIMP) and have used and validated experimentally numerous material models (Chiang, Hieber and Wang, 1991). They detail two variants of the Cross model; a five constant model and a seven constant model. The five constant model is sufficient for the filling stage and the seven constant model for the filling and post filling stages. The five constant model will be used, since only the filling stage is being considered. Also more material data is available on it and it is less complicated than the seven constant model.

In modelling the viscosity, η, experimental results from (Chiang et al, 1991) are used. The shear thinning behaviour of the material in question can be presented by a Cross-type model where the viscosity of the hot melt is given by

$$\eta = \frac{\eta_o}{1 + \left(\frac{\eta_o \dot{\gamma}}{\tau^*} \right)^{1-n}} \tag{3.7}$$

where η_0 is the zero shear rate Newtonian viscosity. This viscosity representation has been shown to work quite well for commercial grade polymer melts. Equation (3.7) is seen to be a two parameter (n,τ^*) model where n corresponds to the power law index and τ^* characterises the shear stress level of the transition region between the Newtonian and power-law asymptotic limits. The simplest reasonably accurate representation of η_0 is in terms of an Arrhenius-type temperature sensitivity and exponential pressure dependence which is given by

$$\eta_o = B e^{T_b/T} e^{\beta p} \tag{3.8}$$

The five constants are n, τ^*, B, T_b, and ß where n and τ^* characterize the shear-thinning behaviour whereas T_b and ß characterize the temperature and pressure dependence of the viscosity. These five constants are unique to the material that is being used in the simulation. Table 3.1 gives a summary of the viscosity model constants for polystyrene (PS) and polypropylene (PP).

Table 3.1 Material constants

Material	PS (678D)	PP(6323)
n	0.274	0.315
τ^*(Pa)	2.31×10^4	1.07×10^4
B (Pa s)	3.04×10^{-9}	5.71×10^{-2}
T_b(K)	13300	5210
β(Pa^{-1})	3.5×10^{-8}	1.5×10^{-8}
Cp (J/Kg°C)	1550	2280
ρ (Kg/m^3)	1012	803
Kt (W/m°C)	0.149	0.196

3.11.2 Overall solution algorithm for non-Newtonian fluids

At this stage of the development the Generalized Hele-Shaw flow equations together with the Volume-of-Fluid method for tracking the free front is solved transiently. A transient scheme gives the actual solution after each time step and hence a finite time step is calculated. With a Newtonian fluid the viscosity remains constant and need not be calculated whereas with a non-Newtonian fluid the viscosity needs to be calculated during each time step.

The algorithm for non-Newtonian thermal flow is detailed as follows:

1. Set all boundary and initial conditions.
2. Solve Equation (3.7) to get the viscosities at all the grid points.
3. Calculate S given by Equation (2.16) at each node using the quadrature formula Eq. (2.26).

4. Solve Equation (2.19) for pressure to give the pressures at the relevant grid points.
5. Repeat steps 2 to 4 till the fractional change in the pressure, temperature and viscosity fields is smaller than a predetermined value ≈ (10^{-4}).
6. Calculate the fluxes given by Equation (2.24) from the pressure distribution.
7. Calculate a new time step, (See Paragraph 3.6), for the time dependant temperature and concentration equations.
8. Solve Equation (2.17) for temperature.
9. Solve Equation (3.1) for concentration.
10. Update boundary values.
11. Repeat steps 2 to 10 till the filling stage is complete.

The filling stage is considered to be complete once the furthest control volume from the point of injection has a concentration value C greater than 0,5 or once the elapsed time equals the calculated filling time.

3.11.3 Non-Newtonian example calculations

Due to the viscosity being highly dependant upon the pressure and temperature of the plastic and hence the position of the free front, it was not logical to incorporate the material model at an earlier stage of the development. In this paragraph some of the simulations of the previous paragraphs are repeated with the material model incorporated. In practice mould designers are only interested in the position of the free front, average temperature field and maximum pressure. The maximum pressure is required for the calculation of the clamping force, the average temperature distribution for the placement of the cooling channels and the position of the free front for the formation of weld lines. In this paragraph the viscosity and shear rate distributions will be presented graphically in the gap

wise direction and discussed in detail. Chiang et al (1991b) published numerous experimental results with which they validate their own finite element code. One of these experiments will be used to validate this finite volume code and the results will be discussed in detail.

The mould geometry, a rectangular cavity of uniform thickness 2,54mm, which Chiang et al (1991 b) used is presented in Figure 3.8. It is preceded by a much thicker rectangular reservoir that gets fed by the runner ensuring that the plastic flows into the mould cavity in an evenly distributed manner causing a flat advancing melt front. The mould is instrumented with three pressure sensors where the positions are indicated on the drawing Figure 3.8. The material used in the experiment is polystyrene (PS) where the material properties are presented in Table 3.1.

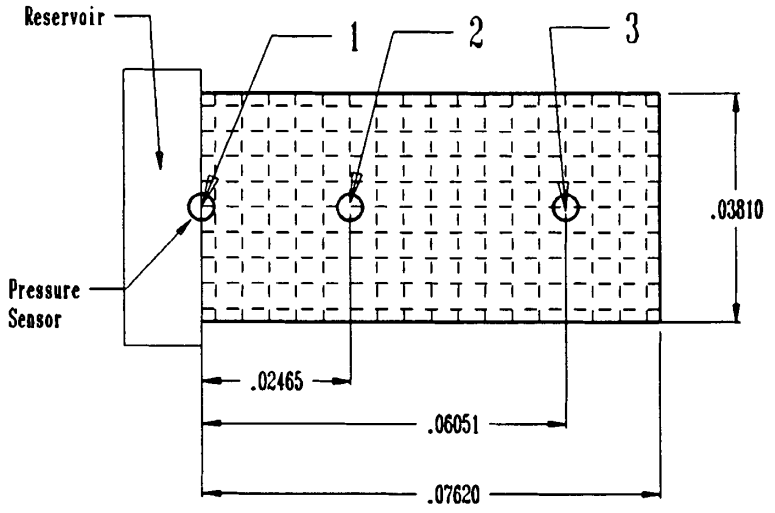

Figure 3.8. Schematic diagram indicating the mould dimensions with the positions of the pressure sensors.

Polystyrene (PS) is injected into the mould at a constant flow rate of 1.07×10^{-5} m^3/s which results in a fill time of 0,69 seconds. The melt temperature is 200°C and the mould temperature 37°C. For the numerical simulation the mould is divided into 19 grid points in the lengthwise direction and 11 grid points in the widthwise direction. This ensures that the control volumes are almost square as shown in Figure 3.8 which results in a favourable aspect ratio and a more accurate solution

The numerical results presented in Figure 3.9 compare favourably with the experimental results presented in Figure 6 (b) of Chiang et al. Due to the nature of this graph it is very difficult to

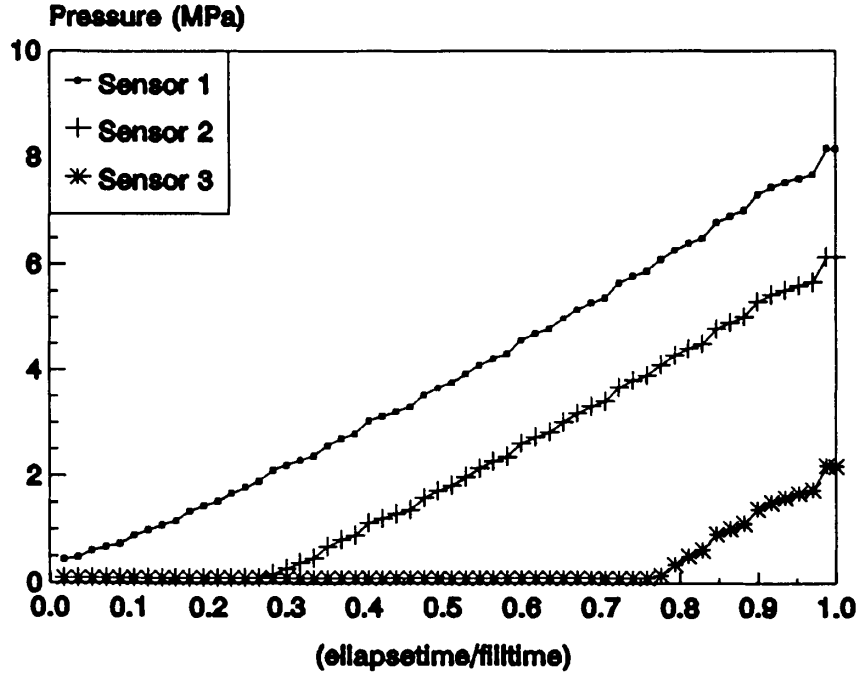

Figure 3.9. Pressure build-up in the mould during filling as indicated by the pressure sensors.

reproduce it. The maximum pressure obtained at the inlet in both cases is more or less 9 MPa. The pressures obtained numerically at fill time at sensors 2 and 3 are identical to the experimental results of 6 MPa and 2 MPa respectively. It is difficult to make a direct comparison throughout filling between the numerical results and the experimental results of Chiang et al (1991) by calculating the errors involved. The results of Chiang are presented in coarse graphical form and any direct comparisons would have to be scaled off his published data which would be meaningless. By comparing the two graphs visually it can be concluded that excellent results are obtained with the finite volume numerical method.

Figures 3.10 to 3.12 present the variables of the Hele-Shaw flow model that vary in the gapwise direction at the positions of the pressure sensors at fill time. The viscosity which characterises the material is dependant upon the temperature and the shear rate. The relationship between these variables is shown by Eqs. (3.7) and (3.8). In addition to the temperature distribution Figure 3.10 also shows how the decline in temperature gradient occurs as a function of the distance from the inlet. Sensor 1 at the inlet shows a steep temperature gradient because the material is all at melt temperature. At sensor 3 a considerable amount of the material close to the wall has started to cool down and the gradient is not as steep as the other two curve's gradients are.

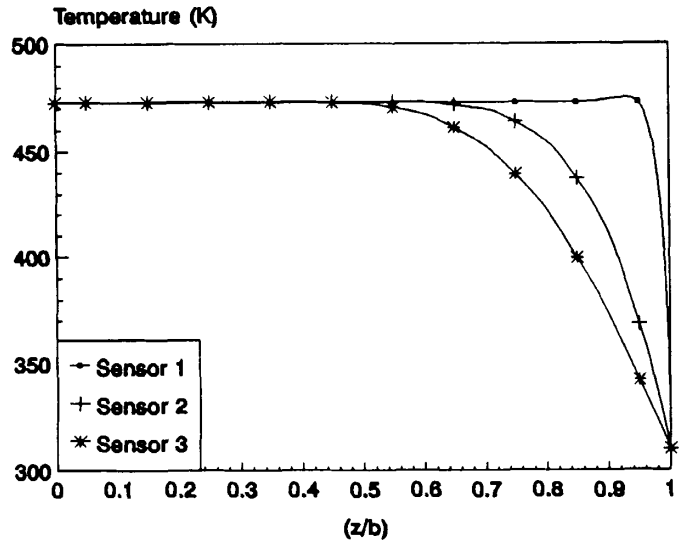

Figure 3.10. Temperature distributions in the gapwise direction at the sensor positions at fill time.

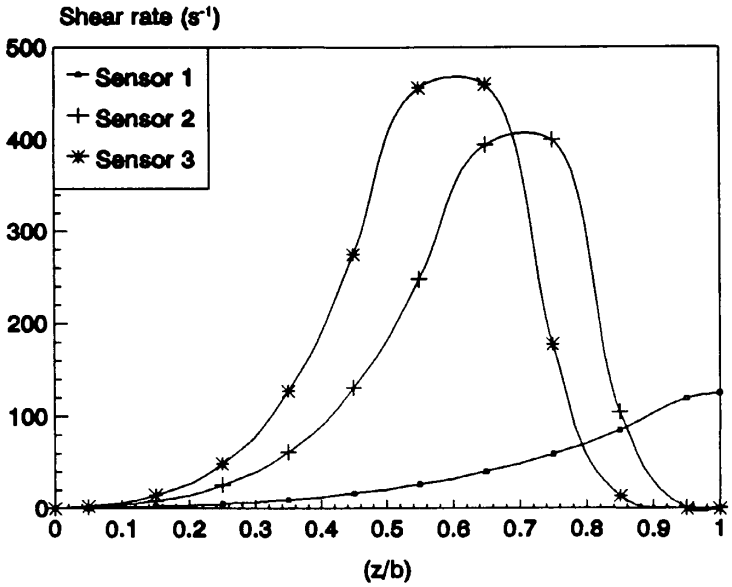

Figure 3.11. Shear rate distributions in the gapwise direction at the sensor positions at fill time.

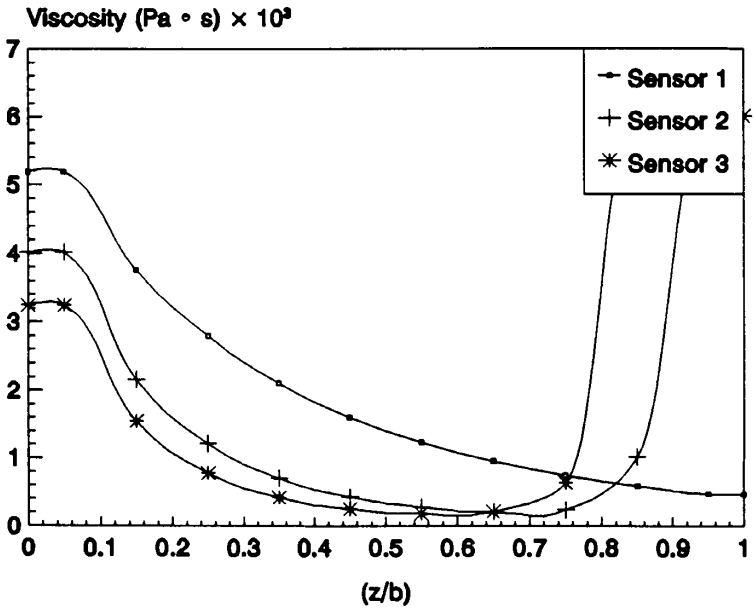

Figure 3.12. Viscosity distributions in the gapwise direction at the sensor positions at fill time.

Figure 3.11 presents the shear rates at the same sensor positions. The definition of the shear rate is given by Equation (2.9). The shear rate is dependant upon the velocity gradients in the gapwise direction. With the numerical method block profiles are assumed for all the variables in the gapwise direction at the inlet and the velocities are no exception. Hence at sensor 1 the shear rate does not vary much in the gapwise direction. The velocity profiles in the gapwise direction within the mould are parabolic and resemble the profile in Figure 2.5. Around the centre line the velocities do not vary much and hence the velocity gradients are not very steep, resulting in low shear rates. Close to the solid boundaries steep velocity gradients occur which give rise to very high shear rates and this can be seen by the graph depicted by sensor 1 Figure 3.11. The graphs depicted by sensors 2 and 3 show that the maximum shear rates are not obtained near the solid walls but at 0,7 and 0,55 of the gap width respectively. The reason for this is that at sensors 2 and 3 the material has already begun to solidify near the solid walls and hence the velocity gradients in these areas are not very steep. By looking at Figure 3.12 it can be seen that in these areas the material's viscosity tends to infinity which means that it has already begun to solidify. At the inlet, even at fill time, it can be seen that the material has not begun to solidify yet because there is a finite viscosity throughout the gapwise direction. By examining Figures 3.10 to 3.12 it can be concluded that the cooler the material the higher the viscosity, the lower the shear rate.

3.11.4 Symmetry test for non-Newtonian thermal flow

As can be seen from Figure 3.12, the non-Newtonian fluid, hot plastic is extremely viscous. The preceding Figures also show that this results in huge pressure, viscosity and temperature gradients which are difficult to simulate without having numerical round-off errors. These errors have a detrimental effect on the overall accuracy of the solution. In Paragraph 2.9.2 the effect of numerical round-off errors is discussed in detail and Figure 2.9 illustrates how the program maintains symmetry on a symmetric domain presented in Figure 2.8 with a constant viscosity. In this Paragraph the

identical test is performed using a non-Newtonian fluid, i.e. with the material model incorporated, and the symmetry is once again investigated.

The same boundary conditions and domain are used for this test except that polystyrene is used in the material model instead of a constant viscosity fluid. The free front has also been incorporated and the program is solved transiently as opposed to iteratively in Paragraph 2.9.2. The incorporation of the free front and material model results in more calculations per iteration and more iterations are required for convergence after each time step. The program being solved transiently requires more calculations because the free front needs to be tracked till fill time is reached in incremental time steps. The results after a particular time step are also the initial values for the next time step and together with the increased number of calculations required numerical round-off errors become an important factor influencing the accuracy of the solution. With this particular investigation the free front is tracked till fill time is reached and then the symmetric pressure distributions along the x and y axes are plotted together with the relative difference between the two as a percentage error.

It can be seen from Figure 3.13 that at the final stage of the Cartesian coordinate version of the program's development the pressure distributions are perfectly symmetric along the x and y axes of Figure 2.8. The percentage error is insignificant at all points. This test proves that the numerical scheme with the free front and material model incorporated is still accurate to within computer accuracy at this final stage of its development.

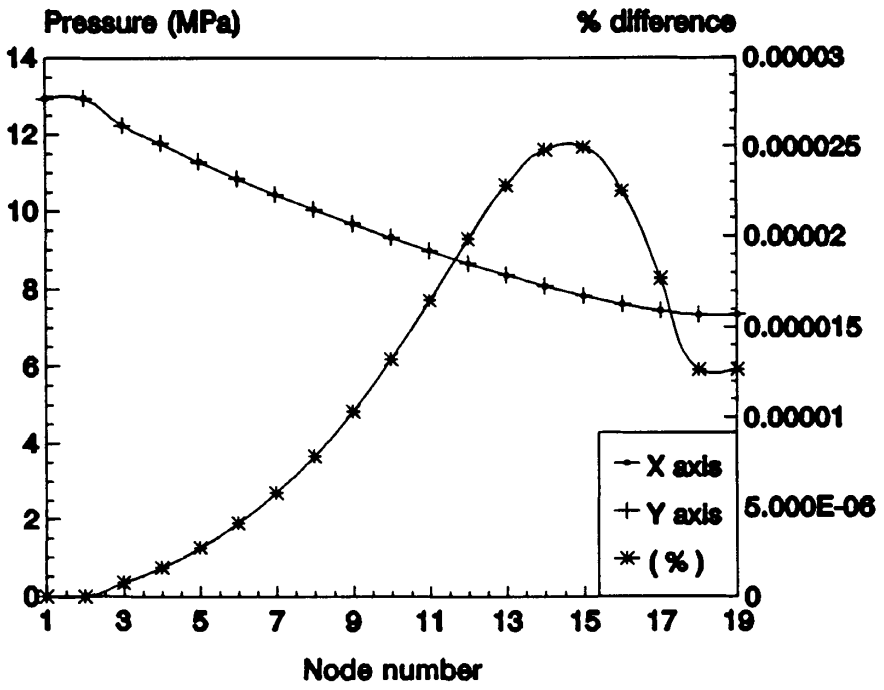

Figure 3.13. Pressure distribution along the x and y axes for the symmetry test with the material model incorporated.

3.11.5 Discretization of the Energy equation

In Paragraph 2.9.3 the effects of using the velocity profiles Eq. (2.7) as opposed to their gapwise average values Eq. (2.8) are investigated for isothermal Newtonian fluid flow without the free front incorporated. Figure 2.10 shows that the difference between the two sets of results is very small. It is also mentioned in Paragraph 2.9.3 that once the free front and the material model is incorporated (thermal non-Newtonian flow) then a difference between the two methodologies could arise.

The development of the material model in Paragraph 3.11 is based upon the gapwise average velocity formulation of the energy equation Eq. (2.8). This formulation requires less memory and is quicker in execution. In this paragraph the effect of the two formulations is investigated for thermal non-Newtonian fluid flow. By looking at Figure 3.14 it can be seen that there is a maximum deviation of 4 percent in the temperature profiles that are generated by the two formulations which is larger than that for isothermal Newtonian flow (see Figure 2.10). By looking at Figure 3.15 it can be seen that this deviation translates into a 0,06 difference in concentration at the position of the free front. Remembering that the position of the free front is at C = 0,5 it can be seen from Figure 3.15 that the deviation in the exact position of the free front is irrelevant. Hence the advantages gained in accuracy by the velocity profile in the energy equation Eq. (2.7) are so slight when compared to the advantages gained in terms of speed and memory usage of the gapwise average velocity Eq. (2.8) formulation, that the latter is recommended for the further development of the program.

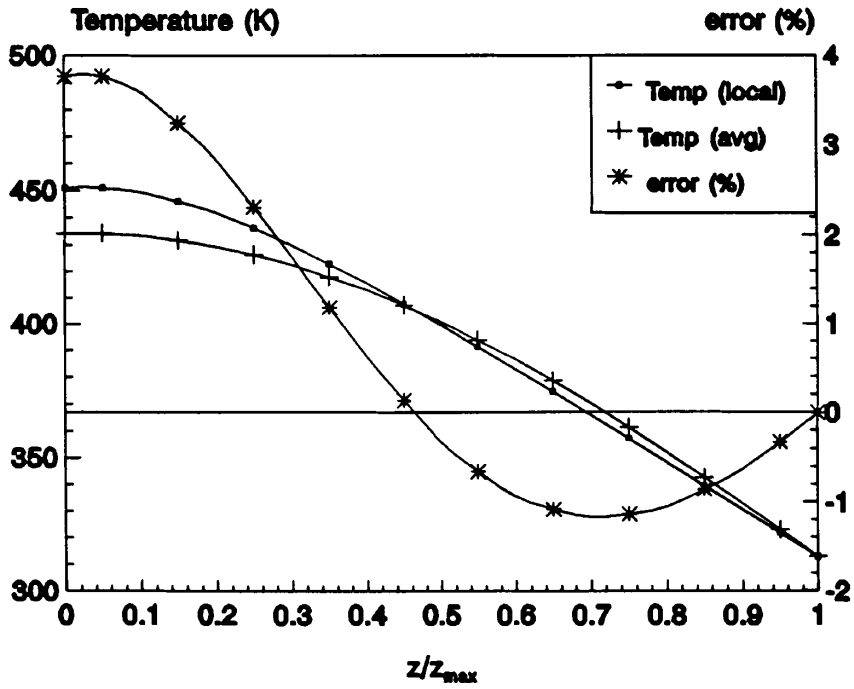

Figure 3.14. Comparing temperature profiles for thermal non-Newtonian flow using gapwise average velocities and velocity profiles.

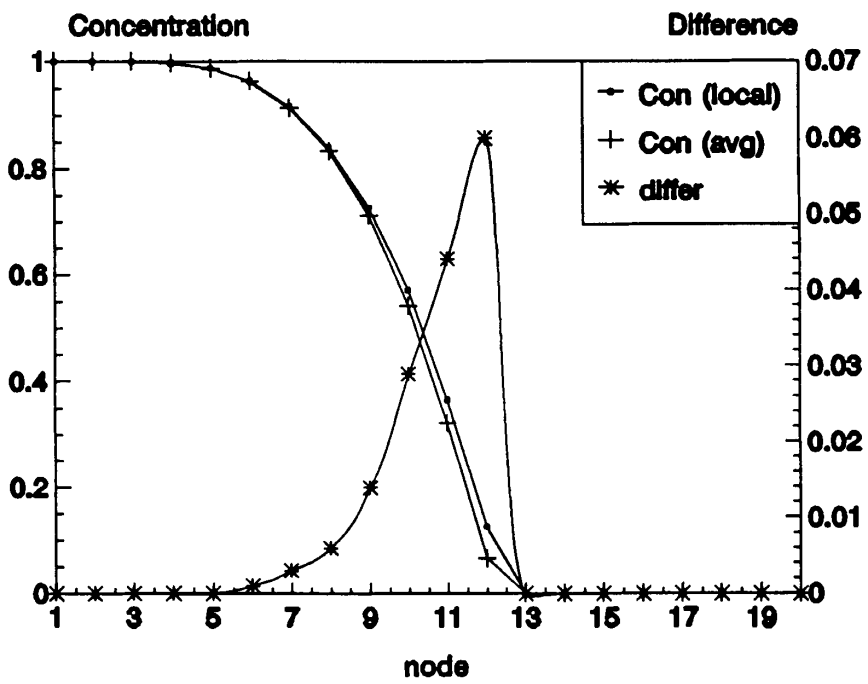

Figure 3.15. Concentration gradient along the centre line for the average velocity versus the local velocity formulation in the energy equation.

3.12 Closure

In this chapter the moving free front algorithm was incorporated into the generalised Hele-Shaw flow model for the simulation of plastics injection moulding. Various models were investigated and the Volume-of-Fluid method was chosen as the one which best suites the objectives of this study. Various methods of discretising the governing equation were proposed and tested numerically. No method distinguished itself as being the best but the hybrid implicit method was recommended. The numerical diffusion problem was investigated and a packing algorithm was developed which sharpened the free front. The existing program was modified to include these developments and was first tested for the

isothermal flow of a Newtonian fluid. After satisfactory results were obtained a suitable material model was added. The results of subsequent simulations were compared to experimental data which had been published and the program was also tested for maintaining symmetry. The different formulations of the energy equation was also investigated with the gapwise average velocity formulation being recommended. All the numerical experiments yielded excellent results. It can be concluded that the Cartesian coordinate version of the generalised Hele-Shaw flow model is producing excellent results and is complete. The next stage of the development is to re-program the flow model for generalised curvilinear coordinates.

4 EXTENSION OF MODEL TO 3-D SHELL VOLUMES

4.1 Introduction

In the previous two chapters the generalised Hele-Shaw flow model for non-isothermal, non-Newtonian flow has been developed to the point where it includes the modelling of the free front. At this stage of the development the finite volume model is restricted by the use of Cartesian coordinates and has only been tested on thin flat rectangular cavities. The results obtained on these domains justify the further advancement of the code to include generalised curvilinear coordinates.

Most polymer processing problems involve flows in domains of irregular shape. While traditional finite difference techniques have many advantages, applying them to irregularly shaped domains requires extensive interpolation and numerical manipulation along the physical boundaries. Such operations are cumbersome, reduce the accuracy of the computation, and make it difficult to develop general purpose codes, whereas finite element methods can easily handle irregularly shaped domains. Finite volume methods can also handle complicated geometries with ease and accuracy using non-orthogonal curvilinear grids which can be generated numerically.

In this chapter the governing equations are transformed to generalised curvilinear coordinates and implemented into the code. This numerical model for plastic injection moulding simulation is verified by simulating the same cases found in the previous chapter. The results obtained from the generalised curvilinear coordinate model are validated against results from the Cartesian coordinate model. The program is then tested on a thin flat trapezoidal geometry. An external numerical grid generation program is also developed for creating structured grids, which act as input data for the Hele-Shaw flow model program, but its development is not discussed.

4.2 Background

The use of generalised curvilinear coordinates is essentially a mapping technique where the physical domain having a complex geometry is mapped into a computational domain having a regular geometry as shown in Figure 4.1. An equivalent problem is then posed in the computational domain by transforming the governing equations into the computational domain using traditional finite differencemethods. The relations are given by a set of partial differential equations which are solved numerically so the mapping procedure itself is mathematical.

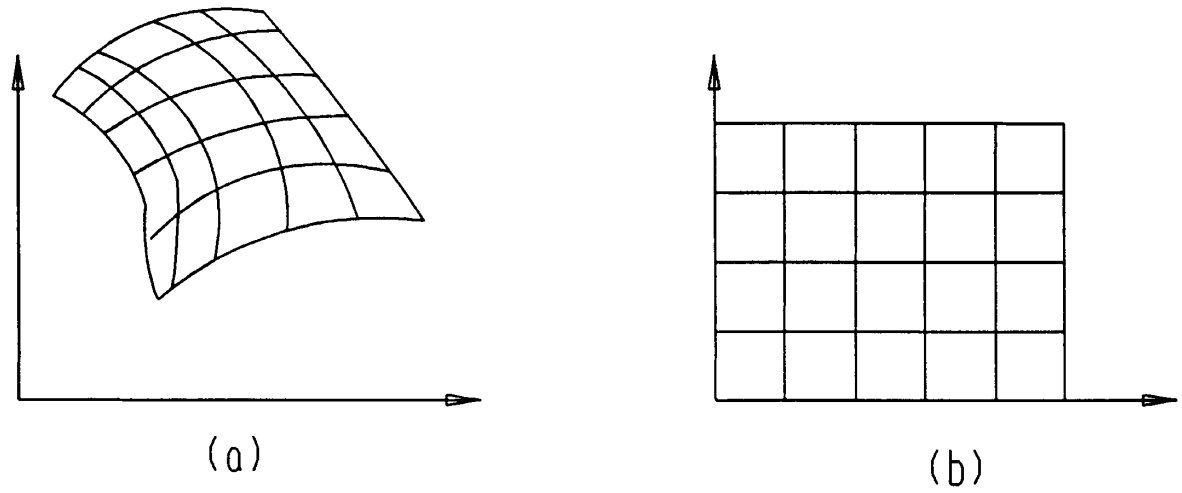

Figure 4.1. Basic nomenclature for (a) physical domain (b) computational domain.

The main difficulty in applying traditional finite difference methods to irregular domains arises from the boundary conditions. With a curvilinear coordinate system the coordinate lines or coordinate surfaces coincide with the boundaries of the physical domain. This makes the representation of the

domain shape and the applying of the boundary conditions easy. Grids can be generated over domains of highly irregular shape. The use of a general non-orthogonal coordinate system combines the geometric flexibility of finite element methods with the computational simplicity of finite difference methods.

The solution of a problem using this methodology involves several steps. First the curvilinear mesh is created over the physical domain. For this a program was developed which generates non-orthogonal grids in complex geometries. It employs transfinite interpolation in conjunction with the solution of a Poison equation to generate boundary fitted curvilinear grids. The method is based on the work of (Thompson, Warsi and Mastin, 1985). Second the governing equations are transformed into the computational domain, i.e. they are rewritten with curvilinear coordinates as independent variables. Third, the governing equations are solved in the computational domain and the results represent those on the equivalent physical domain.

4.3 Transforming the Hele-Shaw equations to generalised curvilinear coordinates

The Hele-Shaw flow equations need to be transformed into the computational domain. Apart from the energy equation, these governing equations are essentially two-dimensional with only the pressure variable being solved. The volumetric flow rate flux components are then derived from the pressure field. This two-dimensional model is now going to be extended with curvilinear coordinates so that it can handle three-dimensional geometries.

The geometries considered in plastic injection moulding (Figure 2.1) are always much thinner in the gapwise dimension (z plane) when compared to the other two dimensions (x and y planes). A three-dimensional part can be unfolded into a thin walled two-dimensional flat plane, hence the transformed

model is considered to be two and a half dimensional. The transformation unfolds the thin walled, three-dimensional component onto a two-dimensional plane. By keeping the gapwise thickness constant the two-dimensional plane dictates the geometrical characteristics of the third dimension for the three-dimensional energy equation. The two-dimensional domain can then be discretized with equal increments in third z dimension. The in plane coordinates x and y are still transformed to match the planar shape of the melt, but the domain is meshed so that the coordinate lines in the z direction do not vary in the x and y directions. Similarly the coordinate lines in the ξ and η do not vary in the z-direction. For simplicity the third coordinate can be kept in terms of z and the transformations carried out only in the x-y plane (Figure 4.1). Hence only the two-dimensional Jacobian will appear in the transformed equations.

A typical control volume in the physical domain is shown in Figure 4.2. The three-dimensional grid points, describing the plane of the thin object, at the principal nodes N,E,W,S are generated externally and imported into the code. The minor nodes ne,nw,se,sw are calculated by a linear interpolation function which obtains the arithmetic mean of the neighbouring nodes. These minor nodes define the control volume and vector notation is used to describe the control volume.

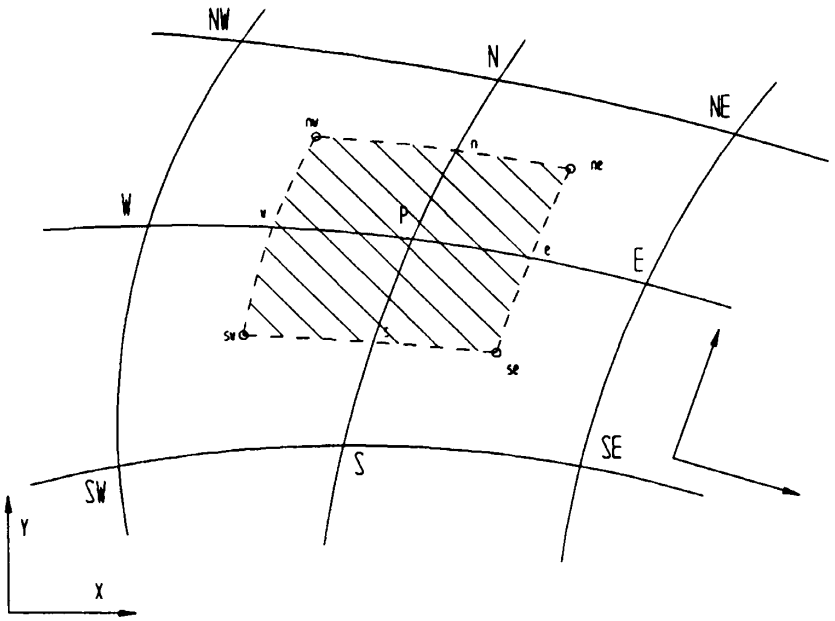

Figure 4.2 Nomenclature for a typical control volume in the physical domain

4.4 Metrics and the Jacobian of transformation

In the transformed equations the independent variables are expressed as functions of the curvilinear coordinates ξ and η which are defined by

$$\left.\begin{aligned} \xi &= \xi(x,y) \\ \eta &= \eta(x,y) \end{aligned}\right\} \qquad (4.1).$$

The field variables (pressure, temperature etc.) retain their definitions from the physical coordinate system, but are now found as functions of the curvilinear coordinates ξ and η instead of as functions of the physical coordinates x and y. It should be mentioned that the form and type of the transformed

equation remains the same as the original partial differential equation: i.e., if the original equation is parabolic, then the transformed equation is also parabolic. In transforming the original equations to curvilinear coordinates the following chain rule is applied.

$$\left.\begin{aligned}\frac{\partial}{\partial x} &= \xi_x \frac{\partial}{\partial \xi} + \eta_x \frac{\partial}{\partial \eta} \\ \frac{\partial}{\partial y} &= \xi_y \frac{\partial}{\partial \xi} + \eta_y \frac{\partial}{\partial \eta}\end{aligned}\right\} \tag{4.2}$$

where $\frac{\delta \xi}{\delta x} = \xi_x$ etc. The derivatives of the curvilinear coordinates with respect to the Cartesian coordinates are known as the metrics. The metrics represent the ratio of arc lengths in the computational space to that of the physical space and are computed in the following manner:

$$\left.\begin{aligned}\xi_x &= J y_\eta \\ \xi_y &= -J x_\eta \\ \eta_x &= -J y_\xi \\ \eta_y &= J x_\xi\end{aligned}\right\} \tag{4.3}$$

where

$$J = \frac{1}{x_\xi y_\eta - y_\xi x_\eta} \tag{4.4}$$

and is defined as the Jacobian of transformation. The physical interpretation of the Jacobian is the ratio of areas in the physical space to that in the computational space. The metrics are determined

numerically from the physical domain where $\Delta\xi$ and $\Delta\eta$ are taken as unity and their nomenclature is presented in Figure 4.3.

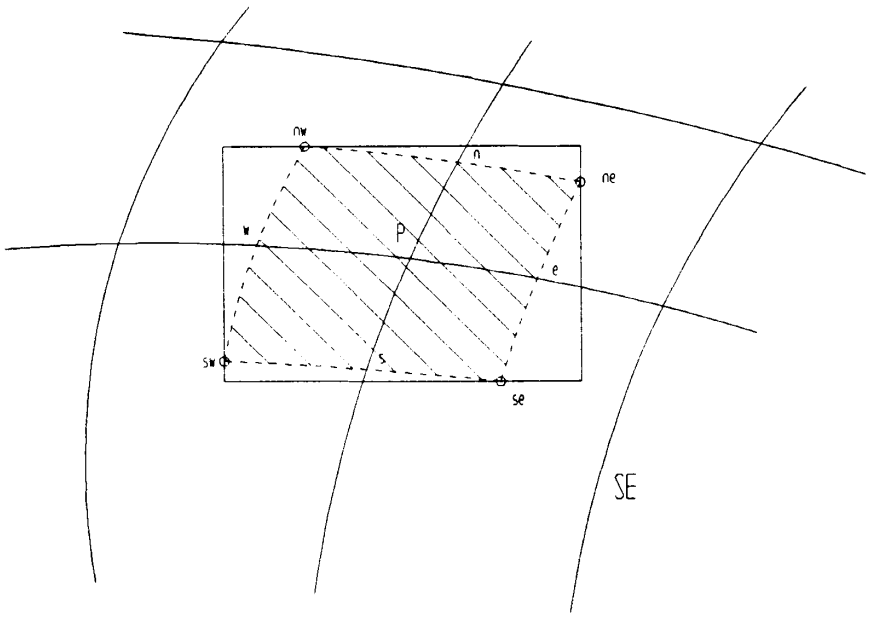

Figure 4.3. Representation of the metrics in the physical domain

4.5 Transformations of the governing equations

In this paragraph the transformation of the generalised Hele-Shaw flow equations will be dealt with. The results of the derivations of the algebraic forms of the partial differential equations (Eq. (2.19)) are conveyed in this section. The fundamental principles behind the transformations including the concept of the flux across the shell volume boundaries will be introduced.

The primary equation behind the Hele-Shaw flow method is the pressure equation (Eq. 2.18) which ultimately has to be transformed to curvilinear coordinates.

$$\frac{\partial}{\partial x}\left(S\frac{\partial p}{\partial x}\right) + \frac{\partial}{\partial y}\left(S\frac{\partial p}{\partial y}\right) = 0 \tag{2.16}$$

In order to transform Equation (2.18), it is written in terms of the thickness averaged continuity equation, Eq. (2.3).

$$\frac{\partial(b\bar{u})}{\partial x} + \frac{\partial(b\bar{v})}{\partial y} = 0 \tag{2.3}$$

With the use of the transformed derivatives Equation (4.2), Equations (2.14) and (2.15) are written in terms of two newly defined variables U and V where U is given by

$$U = b\bar{u} = -S\frac{\partial p}{\partial x} = -S(p_\xi \xi_x + p_\eta \eta_x) \tag{4.5}$$

and V by

$$V = b\bar{v} = -S\frac{\partial p}{\partial y} = -S(p_\xi \eta_y + p_\eta \eta_y) \tag{4.6}$$

U and V are then substituted into Equation (2.3) to obtain Equation (4.7)

$$\frac{\partial U}{\partial x} + \frac{\partial V}{\partial y} = 0 \tag{4.7}$$

Equation (4.7) is then transformed using Equation (4.2) and the technique of Viviand (Anderson, Tannehill and Pletcher, 1984) is applied to obtain

$$\frac{\partial}{\partial \xi}\left(\frac{1}{J}(U\xi_x + V\xi_y)\right) + \frac{\partial}{\partial \eta}\left(\frac{1}{J}(U\eta_x + V\eta_y)\right) = 0 \tag{4.8}$$

where the J is defined in Equation (4.4). The metrics are then replaced with the relations in Equation (4.3) to obtain the final transformed thickness averaged continuity equation

$$\frac{\partial}{\partial \xi}(Uy_\eta - Vx_\eta) + \frac{\partial}{\partial \eta}(Vx_\xi - Uy_\xi) = 0 \tag{4.9}$$

which when integrated across the control volume (Figure 4.2) becomes

$$\begin{aligned}&[(Uy_\eta - Vx_\eta)_e - (Uy_\eta - Vx_\xi)_w]\Delta\eta + \\ &[(Vx_\xi - Uy_\xi)_n - (Vx_\xi - Uy_\xi)_s]\Delta\xi = 0\end{aligned} \tag{4.10}$$

The terms in Equation (4.10) are the volumetric flow rate fluxes that cross the faces of the control volumes and are designated as follows

$$\left.\begin{aligned}F_e &= (U\Delta y_\eta - V\Delta x_\eta)_e \\ F_w &= (U\Delta y_\eta - V\Delta x_\eta)_w \\ F_n &= (V\Delta x_\xi - U\Delta y_\xi)_n \\ F_s &= (V\Delta x_\xi - U\Delta y_\xi)_s\end{aligned}\right\} \tag{4.11}$$

with the metrics defined in Figure 4.3. The discretized equations are then manipulated mathematically and vector notation is introduced to describe the control volumes. Figure 4.4 shows how the control volume shown in Figure 4.2 is described by means of vector notation. The metrics which are displayed in Figure 4.3 are also included in this notation.

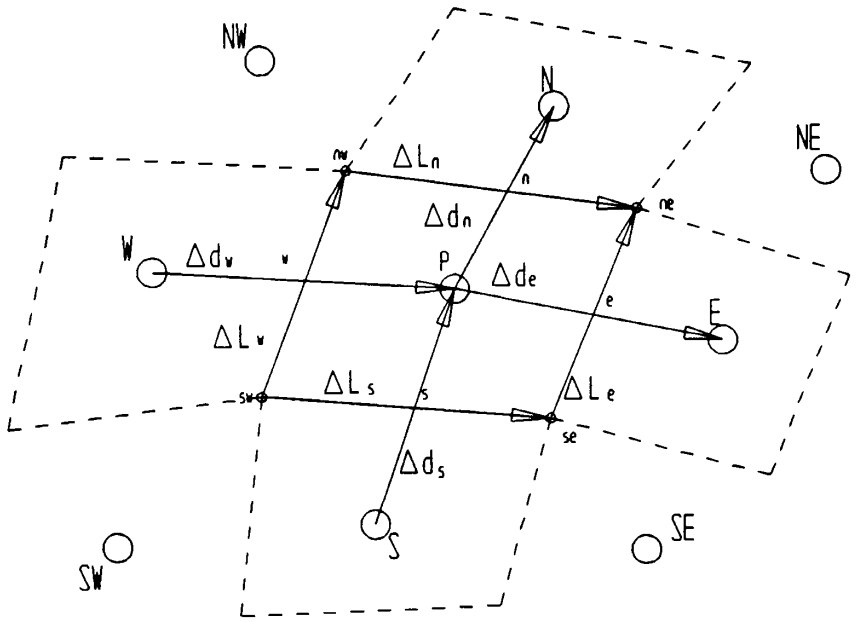

Figure 4.4. A typical control volume indicating the vector notation used.

Mathematical manipulation enables us to simplify the equations with vector algebra which gives rise to the following physical quantities

$$E_j = \left(\frac{\overline{\Delta L} \cdot \overline{\Delta L}}{|\overline{\Delta d} \times \overline{\Delta L}|} \right)_j \tag{4.12}$$

and

$$G_j = \left(\frac{\overline{\Delta L} \cdot \overline{\Delta d}}{|\overline{\Delta d} \times \overline{\Delta L}|} \right)_j \tag{4.13}$$

where these quantities are defined at the surfaces of the control volumes (Figure 4.2) so that j=n,e,w,s in Equations (4.12) and (4.13). Due to the second derivatives that occur in the pressure equation (Eq. 2.18) and the added complexity brought about by the introduction of the generalised coordinates a nine point differential star is introduced in order to solve the pressure field. The direct solver that is used for the Cartesian coordinates can deal with a nine point star without any modifications. The final coefficients for the differential star are given by:

$$\left.\begin{aligned}
A_N &= S_n E_n - \frac{(S_e G_e - S_w G_w)}{4} \\
A_S &= S_s E_s + \frac{(S_e G_e - S_w G_w)}{4} \\
A_E &= S_e E_e - \frac{(S_n G_n - S_s G_s)}{4} \\
A_W &= S_w E_w + \frac{(S_n G_n - S_s G_s)}{4} \\
A_{NW} &= \frac{(S_w G_w + S_n G_n)}{4} \\
A_{NE} &= -\frac{(S_e G_e + S_n G_n)}{4} \\
A_{SW} &= -\frac{(S_s G_s + S_w G_w)}{4} \\
A_{SE} &= -\frac{(S_e G_e + S_s G_s)}{4}
\end{aligned}\right\} \tag{4.14}.$$

EXTENSION TO 3-D SHELL VOLUMES

The energy equation, (Eq. 2.7) is a three-dimensional equation but only the transformations in the x-y plane are considered - see Paragraph 4.3.

$$\rho C_p\left(\frac{\partial T}{\partial t} + u\frac{\partial T}{\partial x} + v\frac{\partial T}{\partial y}\right) = \kappa\frac{\partial^2 T}{\partial z^2} + \eta\dot{\gamma}^2 \tag{2.7}$$

We apply the transformed derivatives Equation (4.2) with the metrics Equation (4.3) to this equation along with the technique of Viviand to obtain the transformed energy equation

$$\begin{aligned}&\frac{1}{J}\frac{\partial(\rho C_p T)}{\partial t} + \frac{\partial}{\partial\xi}(y_\eta(\rho C_p uT) - x_\eta(\rho C_p vT)) + \\ &\frac{\partial}{\partial\eta}(x_\xi(\rho C_p uT) - y_\xi(\rho C_p vT)) = \frac{\partial}{\partial z}\left(\frac{\partial(\kappa T)}{\partial z}\right) + \eta\dot{\gamma}^2\end{aligned} \tag{4.15}$$

This equation is discretized the same as in Chapter 2 but using the flux concept from Equation (4.11) to obtain the following coefficients for the algebraic form

$$\left.\begin{aligned}A_T &= \left(\frac{A_p}{\Delta t} b\,\rho C_p\right)\\ A_N &= \max(0, -\rho C_p F_n)\\ A_S &= \max(0, \rho C_p F_s)\\ A_E &= \max(0, -\rho C_p F_e)\\ A_W &= \max(0, \rho C_p F_w)\\ A_L &= \frac{A_p b\,\Delta\xi\,\Delta\eta}{\Delta Z\,\Delta Z_l}\\ A_U &= \frac{A_p b\,\Delta\xi\,\Delta\eta}{\Delta Z\,\Delta Z_u}\\ S &= \eta\dot{\gamma}^2\Delta\xi\,\Delta\eta\, b\end{aligned}\right\} \tag{4.16}$$

Where A_p is a term that incorporates the Jacobian of the transformation Equation (4.4), and is calculated from the dimensions of the control volume by means of vector algebra. Figure 4.5 presents the vector notation used in calculating A_p which is given by

$$A_p = \overline{B} \times \overline{A} = \frac{\Delta\xi\,\Delta\eta}{J} = \Delta x_\xi \Delta y_\eta - \Delta X_\eta \Delta y_\xi \qquad (4.17).$$

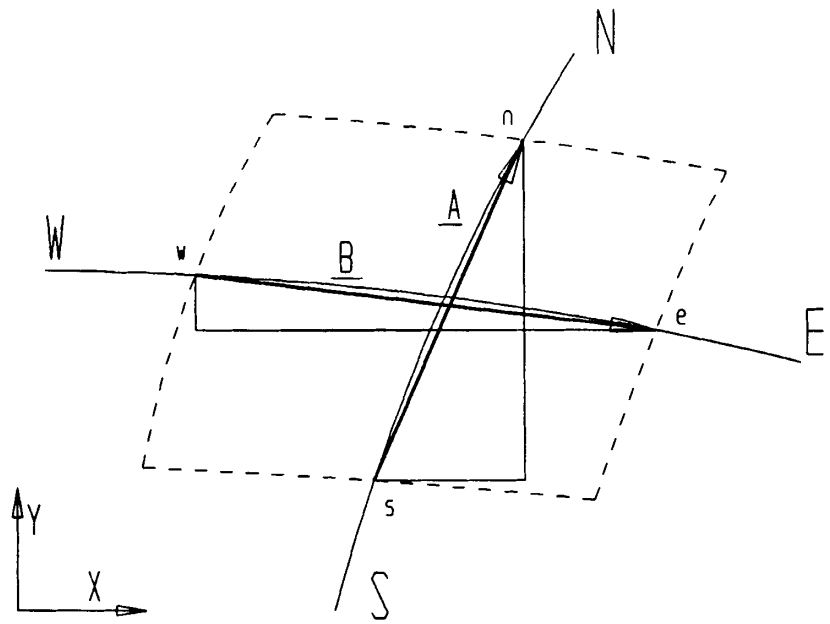

Figure 4.5. Notation used for the calculation of the Jacobian.

The Volume-of-Fluid equation which represents the concentration of the fluid, Equation (3.2), is a two-dimensional equation with single derivatives which makes the transformation straight forward.

$$\frac{\partial C}{\partial t} + \frac{\partial(\bar{u}C)}{\partial x} + \frac{\partial(\bar{u}C)}{\partial y} = 0 \qquad (3.2)$$

Using Equations (4.2) and (4.3) to transform the derivatives with the technique of Viviand the transformed equation is given by:

$$\frac{1}{J}\frac{\partial(\rho C)}{\partial t} + \frac{\partial}{\partial \xi}(\rho \bar{u} C y_{\eta} - \rho \bar{v} C x_{\eta}) + \frac{\partial}{\partial \eta}(\rho \bar{v} C x_{\xi} - \rho \bar{u} C y_{\xi}) = 0 \qquad (4.18)$$

The fluxes that are given in Equation (4.11) are once again used for the discretization and the coefficients for the algebraic form of the partial differential Equation are given by:

$$\left.\begin{aligned} A_t &= \frac{A_p}{\Delta t} \\ A_E &= \max(0, -F_e) \\ A_W &= \max(0, F_w) \\ A_N &= \max(0, -F_n) \\ A_S &= \max(0, F_s) \end{aligned}\right\} \qquad (4.19).$$

Equation (2.16) that is used for the calculation of the S parameter is left unchanged.

These Equations that have been transformed and discretized are now implemented into the code. In the next paragraph identical simulations to those in Chapter 3 will be performed with the aim of verifying the transformations with known results.

4.6 Modifications for the inclusion of the free front and boundaries

When developing the Cartesian coordinate model (Paragraph 3.8) the pressure solving routine had to be modified at the control volumes where the free front was passing through at a particular time

step. The free front moves between the cells in a continuous fashion and does not jump from node to node. The Δx's and Δy's at the position of the free front had to be modified to take the exact position of the front into consideration. This process was called the smoothing of the coefficients.

When using the generalised curvilinear coordinates the same problem occurs at the free front but the smoothing of the coefficients is more complicated. The physical control volume dimensions need to be adjusted at the free front boundary. The control volume's boundaries are adjusted so that the control volume either contains molten plastic or air. No control volume is allowed to contain both. The same linear interpolation function is used to find the exact position of the free front and this is used to modify the vectors defined in Figures 4.4 and 4.5. These vectors are defined in the physical domain and the $\Delta\xi$'s and $\Delta\eta$'s which are the corresponding coordinates in the computational domain also have to be modified so as to include the free front. The $\Delta\xi$'s and $\Delta\eta$'s are usually taken as unity in the equations. The same procedure is used when calculating the pressure gradients across the discontinuous free front. When calculating pressure gradients a vector also has to be defined between the two points. The difference in pressure is taken across the magnitude of this vector.

The technique for defining the control volumes which is explained at the end of Paragraph 4.3 and shown in Figure 4.2 is not valid at the boundaries of the domain. The program has to be adapted so that the correct control volumes are used at the boundaries. This was achieved by modifying the pressure coefficients, Equation (4.14), and the volumetric flow rate fluxes, Equation (4.11) at the boundaries. Since the energy equation and the Volume-of-Fluid equation are directly dependant upon the volumetric flow rate fluxes no modifications are required when solving these equations because the effect of the boundary has already been included.

4.7 Structured versus unstructured grids

The program at this stage of its development can only solve problems on structured grids. A structured grid is a grid resulting from a numerically generated boundary fitted coordinate system grid generation algorithm. This means that the external boundaries of the physical and computational domains have the same number of corresponding node points. Unstructured grids are grids that are generated arbitrarily and each control volume is treated as an independent entity in the program. Each control volume is transformed from its physical domain to its own computational domain and the boundaries of the entire problem are insignificant. Only the boundaries of the control volume in question are important. A program that can deal with unstructured grids is more powerful than a structured grid program because objects (boundaries) in the flow field can be simulated without manipulating the equation coefficients at the particular points. Once this plastic injection simulation code can handle structured grids in an efficient manner it can very easily be extended to include unstructured grids.

4.8 Calculations using the two-dimensional example

4.8.1 Comparing the results to Cartesian coordinate results

In order to ensure that the generalised curvilinear coordinates are incorporated correctly a two-dimensional problem is simulated and verified against the Cartesian coordinate model. The simulation performed in Paragraph 3.11.4 is repeated with both coordinate variants. Once the two variants produce similar results on the rectangular domain Figure 2.8, the generalised curvilinear coordinate model will be tested on a thin flat trapezoidal geometry before a fully three-dimensional problem is attempted.

With this comparison non-isothermal non-Newtonian flow is tested on the square geometry presented in Figure 2.8. The free front is traced until the time step before fill time is reached. The simulation is then interrupted and the pressures along the line of symmetry recorded for both variants, Figure 4.6. The relative difference between the two methodologies is also plotted and represented by means of a percentage difference.

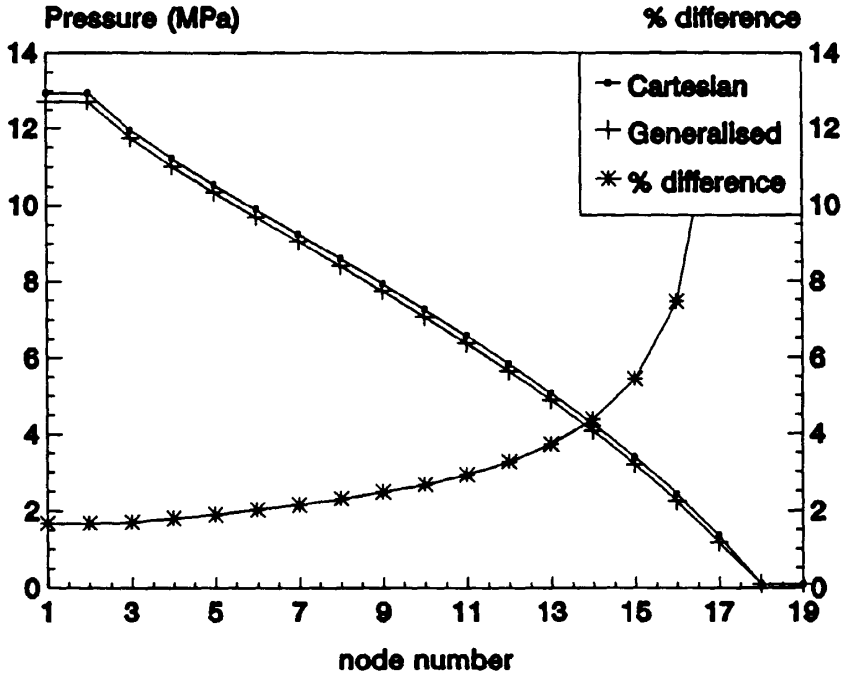

Figure 4.6. Pressure distribution along the line of symmetry for the two coordinate variants.

It can be seen from Figure 4.6 that the Cartesian coordinate model predicts the pressures to be slightly higher than the generalised curvilinear coordinate model does throughout the range at fill time. However by looking at the relative difference between the two it can be seen that the error over

the majority of the field is less than 5 percent. The average percentage difference across the entire field shown in Figure 4.6 is 3.2 percent. These percentage differences are quite acceptable when considering the increased number of calculations per iteration that have to be performed when using the generalised curvilinear coordinate model. From these results it can be concluded that the incorporation of the generalised curvilinear coordinates was successful and the program can be tested on more complex geometries with confidence.

4.8.2 Symmetry tests on the Generalised Curvilinear Coordinate model

In this paragraph the identical symmetry test is applied to the generalised curvilinear coordinate model as what was applied to the Cartesian coordinate model in Paragraph 3.11.4. It was mentioned in Paragraph 4.8.1 that the incorporation of the generalised curvilinear coordinates resulted in more calculations per iteration. With each iteration numerical round-off errors are introduced which could adversely influence the overall accuracy of the entire simulation. The aim of this test is to determine whether the extra calculations introduced by the incorporation of the generalised curvilinear coordinates has a significant influence on the round-off errors. The results for this symmetry test are shown in Figure 4.7.

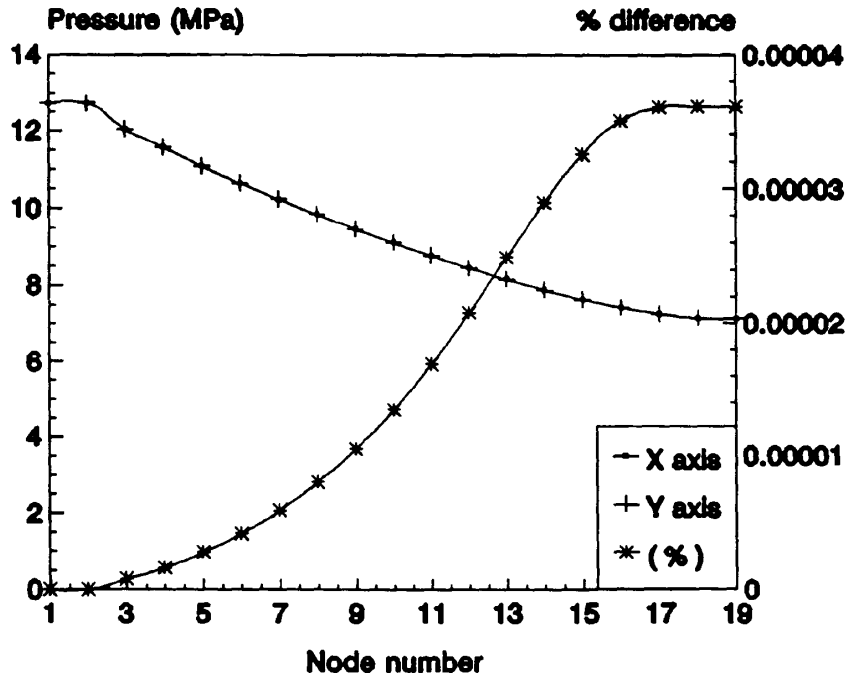

Figure 4.7. Pressure distribution along the x and y axes for the symmetry test with Generalised curvilinear coordinates.

It can be seen from Figure 4.7 that symmetry is maintained. By comparing Figure 4.7 to Figure 3.13 it can be seen that the maximum errors incurred are of the same order of magnitude hence symmetry is still maintained. It can be concluded from Figure 4.7 that the incorporation of the generalised curvilinear coordinates has no adverse effects in maintaining symmetry and the round-off errors which are introduced due to the increase in calculations are insignificant.

4.9 Examples on non-orthogonal two-dimensional grids.

The correlation between the results obtained from the generalised curvilinear coordinate model and the Cartesian coordinate model are within 5 percent of each other on an orthogonal grid. The Cartesian coordinate model cannot deal with non-orthogonal grids and in this paragraph the generalised curvilinear coordinate model will be tested on a non-orthogonal grid. The correlation obtained in the previous paragraph indicates that the generalised curvilinear coordinate model is giving acceptable results on orthogonal grids.

The non-orthogonal grid which will be used for this test is shown in Figure 4.8. Non-Newtonian non-isothermal flow is simulated on a quarter of the mould and the boundary conditions are shown in Figure 2.8. The material that is used in the simulation is polystyrene (PPS), Table 3.1.

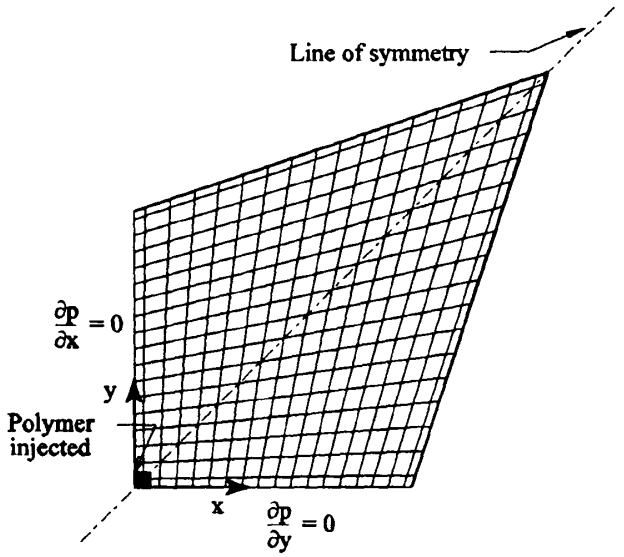

Figure 4.8 Non-orthogonal two-dimensional domain for testing the coordinate transformations.

By looking at Figure 4.9 it can be seen that the two-dimensional non-orthogonal model maintains symmetry. The error is very small and it can be concluded that the additional calculations required when using the generalised curvilinear coordinates have no effect on numerical round-off errors.

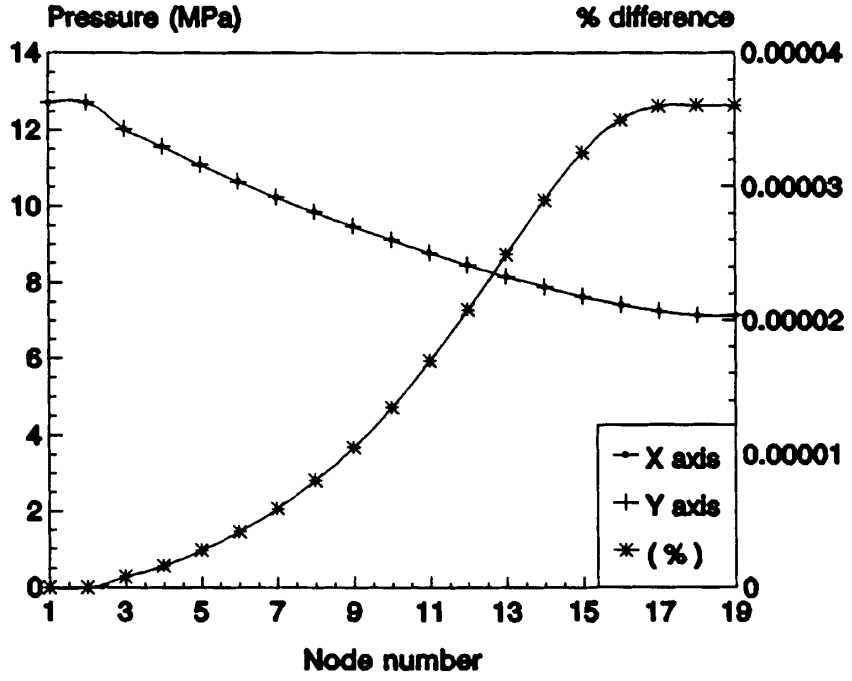

Figure 4.9. Symmetry tests along the two axes of the non-orthogonal two-dimensional model.

Figures 4.10 to 4.12 show the filling stage of the mould at three different time steps. By looking at Figure 4.10 it seems as if the greatest part of the mould gets filled in the first 25% of the filling time. This is not so because the mould gets filled with a constant flow rate and the greater volume of the mould is at its furthest corners. The manner in which the mould is filled is exactly how it is expected

to. Only a quarter of the mould is simulated and the plastic flows the shortest distance to the lowest pressure which is along the x and y axes. Once it has reached the ends of these axes it then chooses the shortest distances to the next lowest pressure positions which happen to be in the corners of the mould. Thus it then flows from the ends of the x and y axes to these corners moving quicker along the solid boundaries than along the plane of symmetry. This explains why the molten material does not flow quicker along the plane of symmetry which one would expect by looking at the contour plots.

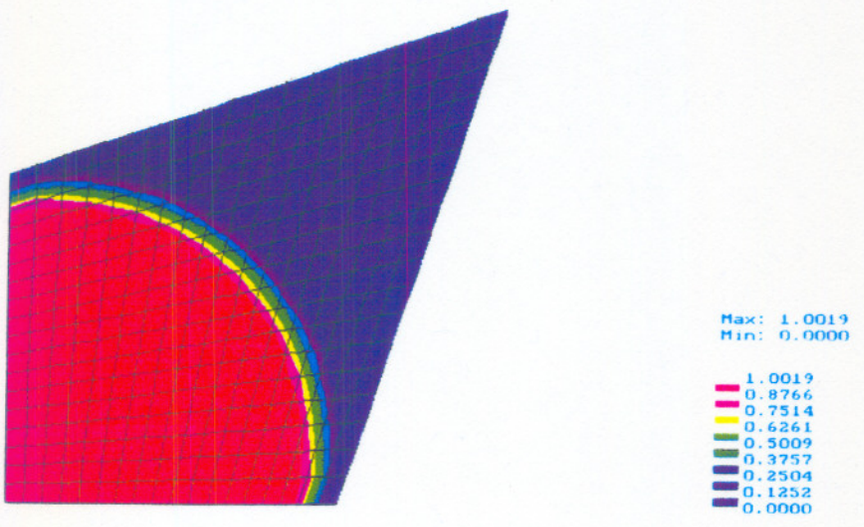

Figure 4.10. Colour contour showing the position of the free front at 0,25 fill time.

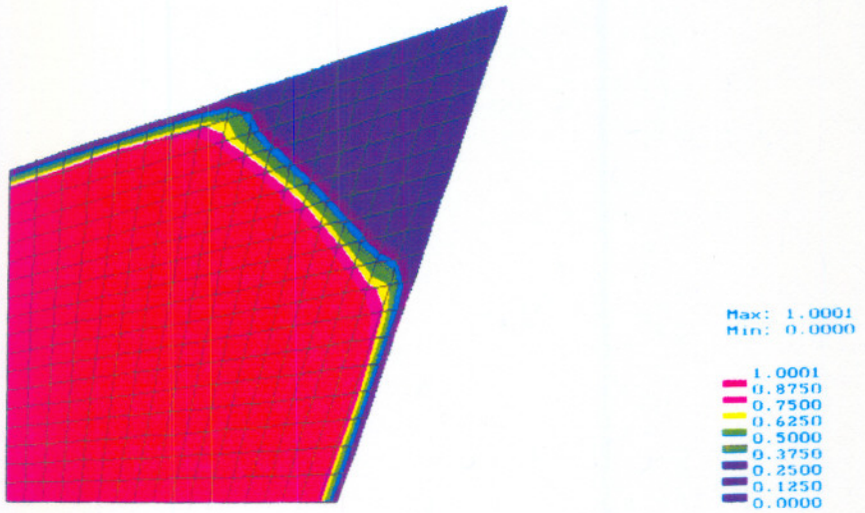

Figure 4.11. Colour contour showing the position of the free front at 0,50 fill time.

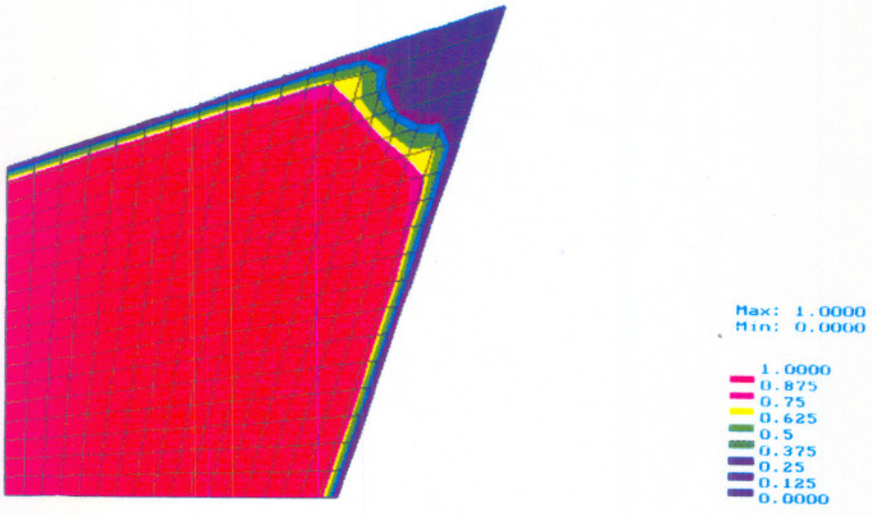

Figure 4.12. Colour contour showing the position of the free front at 0,75 of fill time.

Figure 4.13 shows the average temperature plot in the mould at 50% of the fill time. The material is the hottest at the point where it is injected and cools progressively down, the further it is away from the point of injection. Figure 4.14 is a colour contour plot showing the pressure drop distribution in the mould at 50% of the fill time. At the point of injection the pressure drop is zero and it is the most where the pressure is atmospheric. These results obtained from this colour contour plot are exactly what one would expect.

As a last test the geometry in Figure 4.8 was placed in another plane in the global x-y-z coordinate system and the same simulations were performed. The results obtained were exactly the same as those in Figures 4.10 to 4.14.

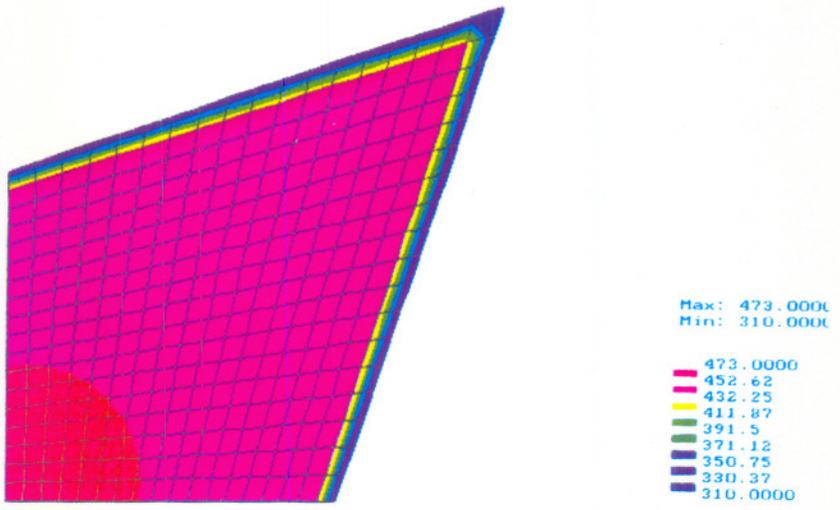

Figure 4.13. Colour contour showing the average temperature distribution at 0,5 of fill time.

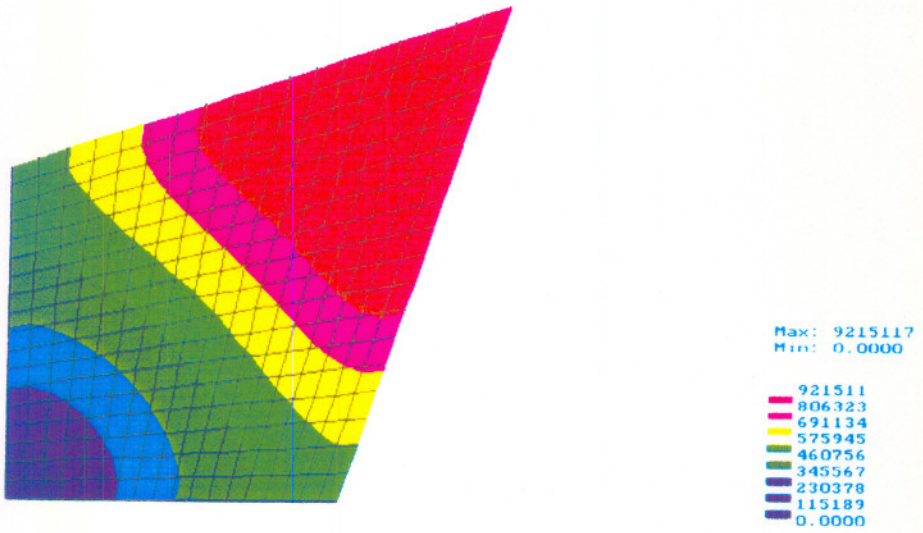

Figure 4.14. Colour contour showing the pressure drop distribution at 0,5 fill time.

4.10 Closure

In this chapter the basic Hele-Shaw algorithm for the simulation of plastic injection moulding, including the free front movement, was extended to include three dimensional shell volumes with generalised coordinates. The governing equations were transformed and the respective differential coefficients were derived and presented. The model was then tested on the same rectangular geometries that were used in Chapter 3 and the correlations were in most cases identical. The three dimensional shell volume code was then applied to a symmetrical two-dimensional non-orthogonal problem varying only in the x-y directions and the results checked for symmetry. The results did conform to symmetry. Colour contour plots were then made of the various variables at different times

during the filling stage and the results obtained were excellent. The same geometry was then placed in a different plane and the same simulations performed. The results were identical indicating the code is correct.

5 CONCLUSIONS AND RECOMMENDATIONS

5.1 Summary.

The conclusions that can be made from this study can be summarised as follows :

i) Numerical models based on the Hele-Shaw flow approximation are well suited to simulate the filling stage of the injection moulding process on a relatively inexpensive personal computer.

ii) The simplicity of the finite volume method used in the generalised Hele-Shaw model makes it an attractive alternative to finite element methods for the simulation of the injection moulding process especially when developing a code for a personal computer.

iii) The Volume of Fluid method can be used successfully in conjunction with finite volume methods in tracking the position of the free front through the domain during the filling stage.

iv) The choice of the material model is not critical and any material model can be implemented. A modified version of the Cross model developed by Wang and Hieber (1988) is used and is recommended.

v) Generalised curvilinear coordinates can successfully be used in conjunction with finite volume methods which enable the finite volume methods to be as powerful as any other method when using irregular geometries.

5.2 Conclusion.

Numerical simulation of the injection moulding process has become a crucial part of advanced injection mould design. Considering the high cost and time required to produce injection moulds, the designer can no longer rely on his experience only. During recent years the need to accurately predict the parameters required in sophisticated injection mould design has been addressed increasingly by the use of computer simulation techniques.

The generalised Hele-Shaw (GHS) model simplifies the numerical simulation of the injection moulding process as compared to a model solving the full Navier-Stokes equations. This enables injection mould simulation codes to be written for the personal computer using less memory and execution time. Most researchers use finite element methods in the numerical schemes employed to simulate the injection moulding process. The finite volume method is very powerful it is not yet been well established for the simulation of the injection moulding process. The simplicity of the finite volume method in solving highly viscous thermal problems has been demonstrated in this thesis. Due to its simplicity it is easier to use than finite element methods. When finite volume methods are used in conjunction with generalised curvilinear coordinates problems involving complex geometries can be solved accurately and quickly. This was also demonstrated in this thesis on structured grids.

The Volume-of-Fluid method was chosen for the tracking of the free front through the domain. It was found that this method was best suited for reaching the objectives of this thesis. It was also found that any material model can be used and a modified Cross model proposed by Wang and Hieber (1988) was incorporated into the code. The choice of material model does not influence the basic numerical model in any way. The material model only provides the non-Newtonian viscosity for a specified temperature and pressure.

5.3 Need for further work.

The next step in this program's development should allow it to solve problems on unstructured grids. This would allow an injection mould which is filled from two or more gates to be simulated around complex internal boundaries known as inserts. After this has been incorporated the program can then be considered for possible commercial development for the filling stage.

It would not be difficult to incorporate the packing stage into this program. It was never the intention of this study to consider the packing stage hence it was not incorporated. The energy equation has already been incorporated into the code and the cooling stage can also be considered. Other factors such as material shrinkage and the sticking of the product to the mould are related to the cooling stage which would also then need to be considered. This study would be complex and require plenty of effort.

There is a need to develop the GHS model further to include the prediction of weld lines which would require an unstructured grid. Weld line prediction is important in the design of plastic products where weld lines influence the aesthetics or the structural strength of the product.

The development work mentioned above covers only a few of the wide range of aspects that can be addressed in the ongoing research work on the numerical simulation of the injection moulding process.

6 REFERENCES

ANDERSON, D.A., TANNEHILL, J.C & PLETCHER, R.H. 1984. Computational Fluid Mechanics and Heat Transfer. New York, Hemisphere, 599 p.

BROYER, E., GUTFINGER, C. & TADMORE, Z. 1975. *A theoretical model for the cavity filling process in injection molding.* Transactions of the Society of Rheology, Vol. 19, Nr. 3, pp. 423-444.

CHIANG, H.H., HIEBER, C.A. & WANG, K.K. 1991a. *A unified simulation of the filling and post filling stages in injection molding. Part I. Formulation.* Polymer Engineering and Science, Vol. 31, Nr. 2, pp. 116-124.

CHIANG, H.H., HIEBER, C.A. & WANG, K.K. 1991b. *A unified simulation of the filling and post filling stages in injection molding. Part II. Experimental Verification.* Polymer Engineering and Science, Vol. 31, Nr. 2, pp. 125-139.

COUNIOT, A., DHEUR, L., HANSEN, O. & DUPRET, F. 1988. A Finite Element Method for Simulating Injection Molding of Thermoplastics. Universitè Catholique de Louvain-la-Neuve, Louvain-la-Neuve, Belgium.

DE KOCK, W.J. 1994. Numerical Simulation of the Plastics Injection Moulding Process. Ph.D. Thesis, University of Cape Town.

DUPRET, F. & VANDERSCHUREN, L. 1988. *Calculation of the temperature field in injection molding.* AIChe Journal, Vol. 34, Nr. 12, pp. 1959-1972.

GREYVENSTEIN, G.P. & LAURIE, D.P. 1994. *A segragared CFD approach to pipe network analysis.* Int. Journal for Numerical Methods in Engineering, Vol. 37, pp. 3685-3705.

REFERENCES

HARLOW, F.H. & WELCH, J.E. 1965. *Numerical calculation of time-dependent viscous incompressible flow of fluid with free surface*. Phys. Fluids, Vol. 8, pp. 2182-2189.

HIEBER, C.A. & SHEN, S.F. 1980. *A finite element, finite difference simulation of the injection molding filling process*. Journal of Non-Newtonian Fluid Mechanics, Vol. 7, Nr. 1, pp. 1-32.

HIEBER, C.A., VANDENENGEL, G. & SHIANG, H.H. 1986. *Cavity-pressure variations during the post filling stage of injection molding*. Annual Technical Conference of the Society of Plastics Engineers, 44th, Boston, USA. Brookfield, pp. 181-184.

HIRT, C.W. & NICHOLS, B.D. 1981. *Volume-of-fluid (VOF) method for the dynamics of free boundaries*. Journal of Computational Physics, Vol. 39, Nr. 1, pp. 201-225.

HOFFMANN. K.A. Computational fluid dynamics for engineers. Austin Texas, Engineering Education System, pp. 243-370

KAMAL, M.R., GOYAL, S.K. & CHU, E. 1988. *Simulation of injection mold filling of viscoelastic polymer with fountain flow*. AIChe Journal, Vol. 34, Nr. 1 pp. 94-106.

KAMAL, M.R. & LAFLEUR P.G. 1982. *Computer simulation of injection molding*. Polymer Engineering and Science, Vol. 22, Nr. 27, pp. 1066-1074.

LAFLEUR, P.G. & KAMAL, M.R. 1986. *A structure-orientated computer simulation of the injection molding of viscoelastic crystalline polymers. Part I. Model with fountain flow, packing, solidification.* Polymer Engineering and Science, Vol. 26, Nr. 1, pp. 92-102.

REFERENCES

LAURIE, D.P. 1983. *Numerical solution of partial differential equations: theory, tools and case studies.* International Series of Numerical Mathematics, Vol. 66, Summer Seminar Series Held at CSIR, Pretoria, February 8-10, 1982, Birkhäuser Verlag, Basel.

NARAZAKI, N. & MIZUKAMI, A. 1990. *Simulation of polymeric flows in the injection molding process.* Convex Users Conference Texas, 1990.

PATANKAR, S.V. 1980. Numerical Heat Transfer and Fluid Flow. Hemisphere, London.

SCHLIGTING, H. 1979, Boundary Layer Theory. 7th Ed New York, McGraw-Hill, 817p.

SHAMES, I.H. 1982. Mechanics of Fluids. 2nd ed. Singapore, McGraw-Hill, 690p.

SPENCER, R.S. & GILMORE, G.D. 1949. *Equation of state for polystyrene.* Journal of Applied Physics, Vol.20, pp. 502-506.

THOMPSON, E. 1986. *Use of pseudo-concentrations to follow creeping viscous flows during transient analysis.* International Journal for Numerical Methods in Fluids, Vol. 6, pp. 749-761.

THOMPSON, J. WARSI, Z & MASTIN, W. C. 1985. Numerical Grid Generation, Foundations and Applications. North Holland Publishers.

WANG, K.K. & HIEBER, C.A. 1987. *A viscosity based simulation of the injection molding process.* In Samanta, S.K., Komanduri, R., McKeeking, R., Chen, M.M. & Tseng, A., eds. Interdisciplinary issues in Materials Processing and Manufacturing, Vol. 2. New York , ASME, pp. 645-660.

WANG, K.K. & HIEBER, C.A. 1988. *Injection molding simulation.* Gutowski, T.G., ed. The Manufacturing Science of Composites, Vol. 4, New York, ASME, pp. 87-94.

WANG, K.K., HIEBER, C.A. & WANG, K.K. 1986. *Dynamic simulation and graphics for the injection molding of three-dimensional thin parts.* Journal of Polymer Engineering, Vol. 7, Nr.1, pp. 21-45.

Abstract

The injection moulding process is one of the most popular means of mass producing components to very small tolerances. Before the advent of the affordable computer, the methods used in injection mould design were empirical in nature. Computational fluid dynamics offers the mould designer a tool to predict and verify the mouldability of a part before any metal is cut on the actual mould. This thesis describes the development of a thin gap numerical model that can be used by mould designers. The thin gap assumption enables the Navier-Stokes equations to be simplified by the Hele-Shaw approximation enabling the flow variables to be solved more efficiently, without a significant loss of accuracy. Finite element solutions of the thin gap model are well documented and are well suited to solving problems with complex geometries but in general finite element methods require more memory and are slower in execution than finite-difference and finite volume methods.

A personal computer based program utilising the finite volume method for solving the Hele-Shaw flow problem is developed in this thesis, which simulates the filling stage of the plastics injection moulding process. The basic model was first developed on a two dimensional constant thickness Cartesian coordinate domain using a constant viscosity. This Newtonian model was then extended with the Volume-of-Fluid method to include the moving boundary or free front. A suitable material model was chosen to predict the viscosities of various grades of plastic at different temperatures and pressures. Once this model produced accurate results it was extended to include generalised curvilinear coordinates in order to solve problems on complex three dimensional geometries. The program is tested and verified extensively with numerical experiments and experimental data from previous published work and excellent results are obtained.

The final product of this thesis is a computer program which simulates the moving boundary during the filling stage of the injection moulding process. This work contributes to the development and understanding of finite volume and finite-difference methods in the simulation of plastic injection moulding.

Uittreksel

Die inspuitgietvormproses is een van die mees gewilde metodes vir die massaproduksie van hoë akkurate produkte. Voor die beskikbaarheid van bekostigbare rekenaars was die inspuitgietvorm ontwerpmetodes hoofsaaklik empiries van aard. Berekeningsvloeimeganika bied die gietvorm-ontwerper 'n gereedskapstuk waarmee hy sy ontwerp kan evalueer voor enige vervaardigingskostes aangegaan word. In hierdie verhandeling word die ontwikkeling van 'n dun- spleet numeriese model beskryf wat deur ontwerpers gebruik kan word. Die Hele-Shaw benadering wat gevolg word is gebaseer op die dunspleet aanname. Hierdie aanname lei tot 'n vereenvoudig van die Navier-Stokes vergelykings wat meebring dat die vloeiveranderlikes baie meer effektief opgelos kan word sonder 'n noemenswaardige verlies aan akkuraatheid. Eindige-elementoplossings van die dunspleet metode is goed gedokumenteer en is veral geskik vir probleme met komplekse geometrië. Eindige-elementmetodes benodig egter meer geheue en is stadiger as beide eindige-verskil- en eindige-volumemetodes.

Hierdie verhandeling beskryf die ontwikkeling van 'n eindige-volumemetode vir die oplos van die Hele-Shaw vloei probleem wat die vulstadium van die plastiekinspuitproses simuleer. Die metode is ontwikkel om binne die beperkings van 'n persoonlike rekenaar te kan funksioneer. Die basiese model was eers op 'n twee-dimensionele konstante dikte Cartesiese gebied ontwikkel met 'n konstante vloeierviskositeit. Hierdie newtoniaanse vloeimodel is toe uitgebrei met die "Volume-of- Fluid" metode om die bewegende vrye front te kan hanteer. 'n Geskikte materiaalmodel is toe gekies om die viskositeite van verskillende tipes plastiek by verskillende temperature en drukke te voorspel. Nadat hierdie program akkurate resultate gelewer het, is dit uitgebrei na algemene kromlynige koordinate om probleme met komplekse drie-dimensionele geometrieë te kan hanteer. Daarna is die program aan die hand van numeriese eksperimente en eksperimentele data van vorige gepubliseerde werk getoets en uitstekende resultate is verkry. Die finale produk van hierdie verhandeling is 'n rekenaar simulasieprogram wat die bewegende rand gedurende die vul stadium van die inspuitgietvormproses simuleer. Hierdie werk dra by tot die ontwikkeling en insig van eindige-volume- en eindige-verskilmetodes in die simulasie van plastiek inspuitvorming.

Acknowledgements

I wish to thank Prof. G.P. Greyvenstein for, despite his busy schedule, guiding this study and promptly giving advice on difficult situations.

I gratefully recognise the contributions which Prof W.J de Kock made in making this thesis possible. When times were tough he was the driving force behind the project.

I wish to thank my family for supporting me during my years of study especially my mother Ann and my father John.

Table of Contents

Nomenclature

Roman alphabet

a	coefficient
A	area
b	half-gap thickness
B	source term
c_p	specific heat
J	Jacobian of transformation
k	thermal conductivity
p	pressure
q	flow rate
s	seconds
T	temperature
t	time
u,v	Cartesian velocity components
V	velocity
x,y,z	Cartesian coordinate directions

Greek alphabet

ζ,η	generalised curvilinear coordinate directions
η	non-Newtonian viscosity
η_o	zero-shear-rate viscosity
γ	shear rate
ρ	density
Δ	increment variation
ϕ	general variable
μ	viscosity

Subscripts

E	grid node right of the one currently under consideration
e	centre of cell face to right of grid node under consideration
l	centre of cell face below grid node under consideration
N	grid node above the one currently under consideration
n	centre of cell face above the grid node under consideration
nb	refers to all four the neighbouring grid nodes
ne	corner of cell to right and above of grid node under consideration
nw	corner of cell to left and above of grid node under consideration
P	refers to the grid node currently under consideration
S	grid node below the one currently under consideration
s	centre of cell face below the grid node under consideration
se	corner of cell to right and below of grid node under consideration
sw	corner of cell to left and below of grid node under consideration
u	centre of cell face above grid node under consideration
W	grid node left of the one currently under consideration
w	centre of cell face to left of grid node under consideration

Superscripts

-	gap-averaged value
t	present time level
t-1	previous time level
.	rate

Abbreviations

CAD	computer aided design
CAM	computer aided manufacture
CAE	computer aided engineering
FAN	flow analysis network
GHS	generalised Hele-Shaw
MAC	Marker-and-Cell
PP	polypropylene
PS	polystyrene
TDMA	tridiagonal matrix algorithm
VOF	fractional volume of fluid

List of Figures

List of Tables